THE MILLIARCSECOND STRUCTURE OF A COMPLETE SAMPLE OF RADIO SOURCES. II. FIRST-EPOCH MAPS AT 5 GHz

T. J. PEARSON AND A. C. S. READHEAD Owens Valley Radio Observatory, California Institute of Technology Received 1987 July 15; accepted 1987 October 20

ABSTRACT

We have conducted a VLBI survey of a complete, flux-density-limited sample of 65 extragalactic radio sources, selected at 5 GHz. We have made 5 GHz images with a resolution ~0.001 of 37 of the sources using the Mark II system, and VLBI images are available for a further five sources. We have classified the sources into a number of groups with similar characteristics, based on the VLBI maps of the sources, their large-scale structure, and their radio spectra.

We have examined the radio polarization, variability, largest angular size, alignment of large-scale and small-scale structure, and optical identification of the sources in each of the classes. One class, compact double sources with steep high-frequency spectra, is distinguished from the other classes by all these criteria: they show low polarization, little variability, and no large-scale structure, and are identified with galaxies. The majority of sources, however, can be grouped into classes that show a regular progression of properties consistent with the increasing prominence of the jet in a "core-jet" structure.

One-sided jetlike structures are found in all classes except the very compact sources and the compact S doubles. No two-sided jets are found. In cases where both a VLBI (parsec-scale) jet and a kiloparsec jet are seen, the VLBI jet is on the same side as, or is connected with, the kiloparsec jet. Large misalignments are common. Superluminal motion is common and has been found in many of the classes, with the notable exception of the compact double sources.

Subject headings: galaxies: jets — interferometry — polarization — radio sources: galaxies — radio sources: general — radio sources: identifications — radio sources: variable

I. INTRODUCTION

The technique of very long baseline interferometry (VLBI) can image the compact radio sources in active galactic nuclei with a resolution 3-4 orders of magnitude greater than can presently be obtained with any other technique at any frequency. The resolution approaches a scale of 1016 cm in nearby galactic nuclei, and permits critical observations that provide new insights into the nature of the central energy source. It is true that VLBI cannot give direct observations of the energy source itself, which may be a supermassive black hole with dimensions 2 or 3 orders of magnitude smaller still than the best available resolution (e.g., Begelman, Blandford, and Rees 1984), and that the radio radiation detected in VLBI observations represents only a small part of the energy output of the central engine (e.g., Phinney 1985). Nonetheless, VLBI is the only available high-resolution imaging technique that can probe active galactic nuclei with subparsec resolution, and such observations have great promise for improving our understanding of the central engines. For example, VLBI observations have already shown that the initial collimation of material ejected from the nuclei takes place on a scale of less than a parsec, and that, at least in some cases, the ejected material is moving at close to the speed of light (e.g., Kellermann and Pauliny-Toth 1981).

VLBI observations have demonstrated that many of the compact radio sources in active galactic nuclei are one-sided jets, and several have shown apparent superluminal motion. But some objects have different morphologies: some are symmetric double sources with an overall extent of less than a kiloparsec, and with no obvious nucleus; some are central components of large, double-lobed radio galaxies or quasars;

and others are steep-spectrum sources with a complex structure. The relationships between the various types of source and the underlying causes of the different morphologies remain unclear. It is not known, for example, whether the morphological differences reflect fundamental differences in the central engines, or are caused by environmental differences in the parent galaxies or the surrounding medium. In order to study these questions, we must first determine the full range of morphological types of compact radio structure and the frequencies with which they occur. Such a study complements the detailed studies of individual sources that are already in progress.

This paper is the second reporting results of a project that we began in 1977 to determine the milliarcsecond structure of a complete sample of radio sources. We chose to observe a fluxdensity-limited sample selected at 5 GHz. The high selection frequency ensures that in many of the objects the dominant radio emission arises in the compact nuclear component. If the radio emission from the compact components is relativistically beamed, the sample may be biased in orientation, with many sources directed toward us. To investigate this possibility, it is important to observe samples such as the one that we have chosen here, which depend to the minimum on theoretical speculation, and also samples in which any possible orientation bias is minimized (Barthel et al. 1984; Cawthorne et al. 1986; Zensus and Porcas 1986; Hough and Readhead 1987). Our approach here has the practical advantage that the sample contains many compact objects that can be studied by Mark II VLBI. The observational selection criteria used for our sample are well defined and allow it to be used for statistical tests of any theories that make quantitative predictions, including the

popular beaming theories. In addition to providing a uniform body of data for statistical studies, our objectives in undertaking this study were to determine the full spectrum of morphologies exhibited by the compact radio sources, and to attempt a physical classification of the morphological types. A further aim was to discover more superluminal sources in order better to determine their statistical properties.

In an earlier paper (Pearson and Readhead 1981, hereafter Paper I) we described the selection of the sample and presented maps of seven sources. This second paper includes first-epoch maps of a further 30 sources, and discusses the properties of the sample as a whole. The observations required to make secondepoch maps of most of the sources have been completed; these maps will enable us to measure changes in the structure of the sources and will be the subject of future papers in the series. Some of the second-epoch results on particularly interesting sources have already been published (Eckart et al. 1985; Pearson et al. 1986; Barthel et al. 1986). In parallel with the radio observations, we are obtaining high-quality optical spectra of all 65 sources in the sample using the Palomar 200 inch (5 m) telescope; some preliminary results have been published (Lawrence et al. 1986, 1987). A program is also underway to measure the optical polarization of all the sources (C. Impey and C. Lawrence, in preparation).

Since the publication of Paper I, we have enlarged the sample from 51 to 65 sources. The revised sample is defined in § II. Forty-five of the 65 sources have milliarcsecond-scale emission detectable with the Mark II VLBI system, and we have undertaken to map all of these, excluding only a few that have been studied by other workers. The observations and the resulting maps are the subjects of § III and § IV, and we attempt to classify the source morphologies in § V. In § VI we discuss some trends and correlations, and in § VII we review the properties of the sources in the various classes and discuss the impact of these results on our physical understanding of these objects. Finally we summarize our conclusions in § VIII. An appendix includes notes on each of the sources and references to other work.

A preliminary report on this work was presented at IAU Symposium 110 (Pearson and Readhead 1984a; Readhead, Pearson, and Unwin 1984), and a more recent summary at the Workshop on Superluminal Radio Sources (Pearson, Readhead, and Barthel 1987).

II. THE COMPLETE SAMPLE

In Paper I we defined a complete sample of 51 sources. Since the publication of Paper I, we have enlarged the sample to 65 sources by removing the northern declination limit. The revised sample is defined by the following criteria: (1) declination (1950.0) $\delta < 35^{\circ}$; (2) Galactic latitude $|b| > 10^{\circ}$; and (3) total 5 GHz flux density $S \ge 1.3$ Jy. The flux densities used in the selection were those measured in the NRAO-MPIfR 6 cm strong source surveys (Pauliny-Toth et al. 1978, hereafter S4; Kühr et al. 1981a, hereafter S5). Since many of the sources are variable, a selection based on flux densities measured at a different epoch would produce a rather different sample. (One source, 1749+701, was measured in both S4 and S5. It is included in the sample on the basis of its S5 flux density, not its S4 flux density, which was below the limit.)

This sample has eight sources in common with a sample of 13 sources that is being studied intensively by a group at the Max-Planck-Institut für Radioastronomie (Eckart *et al.* 1982, 1986, 1987).

The complete sample of 65 sources is listed in Table 1, which gives for each source the name, the 1950.0 coordinates, the nature of the associated optical object, and the redshift where available. The table also gives the date of the mapping observation reported here, the antennas used, and the flux density at the time of observation. Table 1 also includes the fraction F_c of the flux density in a compact core, and the assignment of each source to a morphological class; these entries are discussed in \S V.

Not all the sources in the sample contain a strong, compact component that can be mapped with VLBI. In Paper I we described a "finding survey" in which we detected 35 of the 51 sources south of declination 70°. We subsequently made similar observations of 12 of the 14 northern sources that were added to the sample, and detected 11. (We did not observe two sources, 0210+864 and 1157+732, in which the cores were known to be too weak for VLBI observation.) Thus we detected 46 of the complete sample of 65 sources.

Of these 46 sources, we have completed first-epoch maps of 37, seven of which were published in Paper I. Of the nine sources that we have not mapped, four (3C 147, 3C 179, 3C 236, and 3C 345) have been observed extensively by other workers. The remaining five (0404+768, 0954+556, 0954+658, 1031+567, 1358+624) were detected in the finding survey but were too strongly resolved to be mapped with the US VLBI network; we have observed four of these with the European VLBI network, which has better sensitivity at the required resolution, and we shall report the results elsewhere.

We can make a simple subdivision of the sample sources into two classes, "compact" and "lobe-dominated," based on published observations with resolution ~1". To some extent this division depends on the dynamic range of the observations, but there is a fairly clear distinction between the compact sources dominated by an unresolved core (45 examples in the sample) and the extended sources dominated by emission from lobes (19 examples); one very low-luminosity source (M82) is unusual and does not fit this classification. The 19 lobe-dominated sources can be further separated into three low-luminosity class I sources and 16 high-luminosity class II sources (Fanaroff and Riley 1974). The results of the finding survey can be summarized as follows:

	Total	Detected	Not Detected
Compact sources	45	43	2
Lobe-dominated sources	19	3	16
M82	1	0	1
Total	65	46	19

The three lobe-dominated sources that were detected are class II sources with strong cores (3C 179, 3C 236, and 3C 390.3). The two compact sources that were not detected are both steep-spectrum sources (1634+628 and 2342+821); see the notes in the Appendix.

All 65 sources in the complete sample have been optically identified, and redshifts have been measured for 60 (Lawrence et al. 1987). The sample is dominated by high-luminosity objects; there are a few low-redshift objects (e.g., Markarian 501, 3C 371), but low-luminosity objects such as Seyfert galaxies are very underrepresented compared with a volume-limited sample.

III. OBSERVATIONS

The first-epoch maps of 37 sources were made using the Mark II VLBI system (Clark 1973). Observations were sched-

TABLE 1
THE COMPLETE SAMPLE

Source (1)	Other Designation (2)	R.A. (3)	Decl. (4)	Reference for Cols. (3) and (4) (5)	Optical Identification (6)	V (7)	z (8)	Scale (pc mas ⁻¹) (9)	Reference for Cols. (6) and (8) (10)
0016+731	•••	00 ^h 16 ^m 54 ^s 20	73°10′51″.5	. 1	Q	18	1.781	4.2	1, 2
0040 + 517	3C 20	00 40 19.70	51 47 07.2	2	Ğ	19	0.174	1.9	1
$0108 + 388 \dots$	OC 314	01 08 47.25	38 50 32.8	1	G	22		•••	3
$0133 + 476 \dots$	OC 457	01 33 55.11	47 36 12.8	1	Q	19	0.859	4.2	1, 2
$0153 + 744 \dots$	•••	01 53 04.35	74 28 05.7	1	Q	17	2.338	3.9	1, 2
0210+860	3C 61.1	02 10 40.00	86 05 20.0	2	G	19	0.184	2.0	2, 3
0212+735		02 10 40.00	73 35 40.1	1	Q	19	2.367	3.9	1, 2
0220 + 427	3C 66B	02 20 01.73	42 45 54.6	2	Ğ	12.9	0.0215	0.30	4
0314+416	3C 83.1B	03 14 56.79	41 40 32.6	2	Ğ	12.5	0.0181	0.26	4
0316+413	3C 84	03 16 29.56	41 19 51.9	1	G	11.9	0.0172	0.24	4
				2	G	22			5
0404 + 768	4C 76.03	04 04 00.13 04 54 57.16	76 48 52.5 84 27 53.0	2 1	BL s	18	•••	•••	2
0454 + 844	3C 147	05 38 43.51	49 49 42.8	1	Q	17.8	0.545	3.7	2
$0538 + 498 \dots \dots 0605 + 480 \dots \dots$	3C 153	06 05 44.46	48 04 49.0	2	Ğ	18.5	0.2769	2.6	4
0710+439	OI 417	07 10 03.36	43 54 26.0	1	Ğ	20.7	0.518	3.6	i
0711 + 356	OI 318	07 11 05.60	35 39 52.6	1	Q	17	1.62	4.2	2
0723 + 679	3C 179	07 23 04.29	67 54 52.7	2	Q	18.0	0.846	4.2	2 2
0804 + 499	OJ 508	08 04 58.40	49 59 23.1	1 2	Q	17.5 17.8	1.43	4.3 4.2	$\frac{2}{2}$
0809 + 483	3C 196 OJ 425	08 09 59.42	48 22 07.2 42 32 07.7	2 1	Q BL	17.8 17.7	0.871		5
0814 + 425		08 14 51.67							
$0831 + 557 \dots$	4C 55.16	08 31 04.38	55 44 41.4	1	G	17.5	0.2420	2.4	4
$0836 + 710 \dots$	4C 71.07	08 36 21.56	71 04 22.4	1	Q	16.5	2.17	4.0	2
$0850 + 581 \dots$	4C 58.17	08 50 50.15	58 08 55.7	1	Q	18	1.322	4.3	2
$0859 + 470 \dots$	4C 47.29	08 59 39.98	47 02 56.8	1	Q	18.7	1.462	4.3	2
0906 + 430	3C 216	09 06 17.25	43 05 59.4	2	Q	18.5	0.67	3.9	2
$0917 + 458 \dots$	3C 219	09 17 50.66	45 51 43.6	3	G	17.2	0.1744	1.9	4
$0923 + 392 \dots$	4C 39.25	09 23 55.32	39 15 23.5	1	Q	17.9	0.699	4.0	2
$0945 + 408 \dots$	4C 40.24	09 45 50.08	40 53 43.4	1	Q	17.5	1.252	4.3	2
$0951 + 699 \dots$	M82 (3C 231)	09 51 41.95	69 54 57.5	2	G	8.4	0.0009	0.013	4
$0954 + 556 \dots$	4C 55.17	09 54 14.36	55 37 16.4	1	Q	17.7	0.909	4.2	2
$0954 + 658 \dots$		09 54 57.85	65 48 15.5	1	BL	16.7	0.368	3.1	1, 2
1003 + 351	3C 236	10 03 05.39	35 08 48.0	2	G	16.0	0.0989	1.2	4
$1031 + 567 \dots$	OL 553	10 31 55.96	56 44 18.1	1	G	21.3	0.45	3.4	3, 5
$1157 + 732 \dots$	3C 268.1	11 57 49.89	73 17 27.5	4	G	21.5	0.97	4.2	. 6
$1254 + 476 \dots$	3C 280	12 54 41.05	47 36 32.1	2	G	20	0.994	4.3	7
1358 + 624	4C 62.22	13 58 58.36	62 25 06.7	1	G	20.9	0.431	3.3	1
1409 + 524	3C 295	14 09 33.50	52 26 13.0	2	G	20.1	0.4614	3.4	4
1458 + 718	3C 309.1	14 58 56.64	71 52 11.2	2	Q ,	16.8	0.905	4.2	2
$1609 + 660 \dots$	3C 330	16 09 16.16	66 04 30.0	2	G	20.3	0.549	3.7	4
1624 + 416	4C 41.32	16 24 18.25	41 41 23.5	1	Q	22	2.55	3.8	3
1633 + 382	4C 38.41	16 33 30.63	38 14 10.0	1	Q	18,	1.814	4.2	2
1634+628	3C 343	16 34 01.08	62 51 41.6	ī	Ò	20.6	0.988	4.3	2
1637 + 574	OS 562	16 37 17.43	57 26 15.7	1	Ò	17	0.745	4.1	2
1641 + 399	3C 345	16 41 17.61	39 54 10.8	1	Q	16.0	0.595	3.8	2
$1642 + 690 \dots$	4C 69.21	16 42 18.08	69 02 13.2	1	Q	19.2	0.751	4.1	1, 2
1652 + 398	4C 39.49	16 52 11.73	39 50 25.1	4	G	13.8	0.0337	0.46	2
1739 + 522	4C 51.37	17 39 29.00	52 13 10.4	i	Q	18.5	1.375	4.3	2
1749 + 701		17 49 03.40	70 06 39.6	1	ВĹ	17.0			2
$1803 + 784 \dots$.1.	18 03 39.18	78 27 54.3	1	Q	17	0.68	4.0	2, 3
$1807 + 698 \dots$	3C 371	18 07 18.54	69 48 57.1	1	G	14.2	0.050	0.67	2
1823 + 568	4C 56.27	18 23 14.95	56 49 18.1	1	BL	18.4	0.664	3.9	1, 2
1828 + 487	3C 380	18 28 13.54	48 42 40.5	2	Q a	16.8	0.692	4.0	2
1842 + 455	3C 388	18 42 35.45	45 30 21.6	2	Ğ	15.3	0.0908	1.1	4
1845 + 797	3C 390.3	18 45 37.57	79 43 06.4	$\frac{1}{2}$	Ğ	15	0.0569	0.75	4
1928 + 738	4C 73.18	19 28 49.35	73 51 44.9	1	Q	16.5	0.302	2.8	1, 2
1939 + 605	3C 401	19 39 38.84	60 34 32.6	2	G	18.0	0.201	2.1	4
1954 + 513	OV 591	19 54 22.47	51 23 46.4	1	Q	18.5	1.22	4.3	2 2
2021 + 614	OW 637	20 21 13.30	61 27 18.1	1	Ğ	19.5	0.2266	2.3	8
2153 + 377	3C 438	21 53 45.49	37 46 12.9	2	Ğ	19.2	0.292	2.7	4
2200 + 420	BL Lac	22 00 39.36	42 02 08.6	1	BL	14.5	0.07	0.90	2
					G		0.0171		4
2229 + 391	3C 449	22 29 07.60	39 06 03.4 30 25 27 6	2 2	G	13.2 16.0	0.0171	0.24 1.0	4
$2243 + 394 \dots 2342 + 821 \dots$	3C 452	22 43 32.81 23 42 06.35	39 25 27.6 82 10 01.3	5	Q , t	20.5	0.735	4.0	3
4J74 T 041									
2351 + 456	4C 45.51	23 51 49.96	45 36 22.9	2	Q	20.6	2.0	4.1	3

TABLE 1—Continued

VLB? (11)	Mapped (12)	Antennas (13)	S _t (14)	S ₀ (15)	F _c (16)	Classification (17)
Y	1982 Apr	BKGFO	1.65	1.7	0.95	Very compact
N			4.18		< 0.003	F-R II
Y	1979 Jul	GFOH	1.35	1.6		Compact S double
Y	1978 Dec 1982 Apr	GFOH BGFO	3.26 1.51	1.8 1.5	0.89	Compact F double
	-	boro				
N Y	1980 Sep	BKFO	1.68 2.20	2.3	< 0.007 0.59	F-R II Asymmetric I
Ň	1700 БСР		3.75		< 0.06	F-R I
N			3.53		< 0.01	F-R I
Y	1978 Dec	GFOH	47.2	57.	•••	Irregular
\mathbf{Y}^{-1}			2.79		0	Steep-spectrum compact
Y	1981 Aug	BKGFO	1.40	1.0	0.51	Asymmetric I
Y	•••	•••	8.18	•••		Steep-spectrum compact
N Y	1980 Jul	BKGFO	1.35 1.66	1.6	< 0.004	F-R II Compact S double
Y Y	1980 Jul	BKGFO	1.51 1.31	1.1	0.24 0.31	Compact F double F-R II
Y	1979 Dec	BKGFO	2.07	 1.4	0.31	Very compact
N			4.35		< 0.012	F-R II
Y	1979 Jul	GFOH	1.68	1.9	0.84	Compact
Y	1979 Dec	KGFO	5.60	5.3	*	Irregular
Y	1980 Sep	BKFO	2.57	2.6	0.40	Asymmetric II
Y	1980 Jul	BKFO	1.41	1.1	0.85	Compact
Y	1978 Dec	GFOH	1.78	1.7	0.68	Asymmetric I
Y	1979 Dec	BKGFO	1.78	1.9	0.45	Steep-spectrum compact
N			2.29		< 0.018	F-R II
Y Y	1978 Dec 1979 Jul	GFOH GFOH	8.90 1.39	7.5 1.5	0.48	Compact F double
N	19/9 Jul		3.94	1.5	0.46	Asymmetric II (Not classified)
Ÿ			2.27			(Not observed)
Y			1.46			(Not observed)
Ÿ			1.32		< 0.28	F-R II
Y			1.31			(Not observed)
N	•••	•••	2.63	• • •	< 0.015	F-R II
N	•••	•••	1.53	• • • • • • • • • • • • • • • • • • • •	< 0.007	F-R II
Y		•••	1.77	• • •		(Not observed)
N Y	1001 Ana	BKGFO	6.48 3.34	3.3	<0.009 0.18	F-R II
N	1981 Aug	bkGFO	2.35		< 0.13	Steep-spectrum compact F-R II
Y	1980 Jul	BKGFO	1.31	1.2	0.35	Asymmetric II
Y	1979 Apr	BKGFO	4.08	2.3	0.37	Asymmetric II
Ň			1.50		0	Steep-spectrum compact
Y	1979 Jul	GFOH	1.44	1.9	0.96	Very compact
Y			10.9	7.5	0.35	Asymmetric II
Y	1980 Jul	BKGFO	1.43	1.9	0.86	Compact
Y	1980 Jul	BKGFO	1.42	1.3	0.35	Asymmetric II
Y Y	1982 Apr 1982 Apr	BGFO BKGFO	1.99 1.81	1.0 1.3	0.91 0.67	Very compact Asymmetric I
Y	1982 Apr	BKGFO	2.63	2.9	0.74	Asymmetric I
Ŷ	1978 Dec	GFOH	2.33	2.4	0.40	Asymmetric II
Y	1979 Dec	BKGFO	1.67	1.5	0.74	Asymmetric I
Y	1978 Dec	GFOH	6.19	3.0		Steep-spectrum compact
N		•••	1.77		< 0.03	F-R II
Y	1982 Apr	BKGFO	4.32	2.3	0.13	F-R II
Y	1980 Sep	BKFO	3.34	3.3	0.64	Asymmetric I
N			1.52		< 0.028	F-R II
Y	1979 Jul	GFOH	1.43	1.5	0.57	Asymmetric I
Y N	1979 Dec	KGFO 	2.31 1.54	2.2	< 0.007	Compact F double F-R II
Y	1978 Dec	GFOH	4.75	2.3	0.52	Asymmetric I
N			1.39		< 0.027	F-R I
N N			3.26		< 0.027 < 0.04	F-R II
N			1.30			Steep-spectrum compact
Y	1980 Jul	BKGFO	1.41	1.1	0.29	Asymmetric II
Y	1979 Dec	BKGFO	1.77	1.6	0.45	Compact S double

uled by the US VLBI network in seven sessions between 1978 and 1982 (Table 2). Most sources were scheduled to be observed continuously for about 11 hours using five antennas (four antennas of the US network and the 100 m antenna of the Max-Planck-Institut für Radioastronomie at Effelsberg), but owing to a variety of technical problems not all the observations were successful, so the coverage of the (u, v)-plane obtained varied considerably from source to source. Table 2 gives details of the observations of each source. The typical resolution is 1-2 mas $(1 \text{ mas} = 0.001 = 4.85 \times 10^{-9} \text{ radians})$.

The data were cross-correlated on the Caltech-JPL Mark II VLBI processor. Estimates of the cross-correlation coefficients were obtained by a least-squares fit on each baseline independently; in most cases a coherent integration time of 120 s was used (Table 2). The "global fringe-fitting" procedure (Schwab and Cotton 1983) was not used. The data were calibrated in the usual way (Cohen et al. 1975) using measurements of antenna system temperatures and either antenna temperatures or antenna gain curves. The a priori amplitude calibration was adjusted in some cases to achieve agreement at baseline crossing points in the (u, v)-plane; in the later observations, the calibration was further improved by using a self-calibration technique.

Images of the sources were obtained by model fitting and hybrid mapping methods. Most of the sources had a fairly simple brightness distribution that could be well represented by a simple model consisting of one, two, or three elliptical Gaussian components. The model parameters were initially guessed by inspection of the visibility amplitudes and closure phases, and then improved estimates were made by an iterative least-squares fitting program. The Gaussian model was used as a starting model for an iterative self-calibration and mapping procedure (Pearson and Readhead 1984b). The art of VLBI image reconstruction has progressed rapidly in the years since this project was begun. The earliest images were made by the method of Readhead and Wilkinson (1978) that uses selfcalibration of visibility phases only; in later observations, amplitude self-calibration was also applied using an adaptation by S. C. Unwin of the CORTEL program (Cornwell and Wilkinson 1981). Thus the quality of the resulting images varied, depending on the extent of the (u, v)-plane coverage and the analysis methods used. Typically the dynamic range of the images (the ratio of the brightness of the brightest feature in the

map to the rms noise in an area of blank sky) varied from about 50:1 for observations with four antennas and without amplitude self-calibration to about 300:1 for observations with five antennas and amplitude self-calibration. It is clear that in many cases it would be possible to achieve an improvement in image quality by reanalyzing the data, but it is unlikely that such an effort would result in substantial changes in the apparent structure of the sources. We shall reanalyze the data presented here using the best available methods when we analyze the second-epoch observations (in preparation). The second-epoch maps should in most cases be greatly superior to the first-epoch maps, owing both to improved analysis methods and to the use of more antennas.

IV. RESULTS

The resulting VLBI images of 37 sources are presented as contour maps in Figure 1. For completeness, we include the seven maps published in Paper I. All the images have been restored with Gaussian clean beams, the FWHM contours of which are shown as hatched ellipses in Figure 1. The parameters of the restoring beam, the peak brightness, and the contour levels used for each map are listed in Table 3.

The notes on each source in the Appendix draw attention to interesting features of the VLBI images and discuss their relationship to other observations. References are given to observations of the sources that were not mapped in this project.

The contour maps are not the most convenient presentation of the data for quantitative analysis. In Table 4 we present the parameters of Gaussian models of all but the most complex sources. In cases where self-calibration was used to make the maps, these models were derived by least-squares fitting of the self-calibrated data. The agreement factors (reduced χ^2) in columns (8) and (9) indicate the quality of the fit. When the agreement factor is less than 2, the model is a moderately accurate representation of the source structure; larger agreement factors indicate that the model is overly simple.

We have not attempted to estimate errors in the model parameters. The best-determined parameters are the flux densities and relative positions of well-separated, barely resolved components; in such cases the positions should be accurate to $\lesssim 0.1$ beamwidth (i.e., 0.1 mas in most cases). When two or more components are blended, the uncertainties are greater

Notes to Table 1

```
Col. (1).—Source name according to IAU convention.
```

Col. (2).—Alternative source name.

Col. (3).—Right ascension (1950.0).

Col. (4).—Declination (1950.0).

Col. (5).—Reference for radio position in cols. (3) and (4): (1) Perley 1982; (2) Peacock and Wall 1981; (3) Perley et al. 1980; (4) VLA position (R. A. Laing and R. A. Perley, private communications); (5) Peacock and Wall (VLA position; 1985, private communication).

Col. (6).—Optical identification: G = galaxy, Q = quasar, BL = blazar. The distinction between Q and BL is sometimes unclear.

Col. (7).—Approximate visual magnitude of the optical object.

Col. (8).—Redshift.

Col. (9).—Linear scale (pc mas⁻¹), assuming $H_0 = 100 \,\mathrm{km \, s^{-1} \, Mpc^{-1}}$ and $q_0 = 0.5$.

Col. (10).—Reference for optical identification and redshift: (1) Lawrence et al. 1986; (2) Hewitt and Burbidge 1987; (3) unpublished work by C. R. Lawrence, S. C. Unwin, and the authors (see also Lawrence et al. 1987) [0108 + 388, 1624 + 416; 1803 + 784; 2342 + 821, 2351 + 456]; (4) Burbidge and Crowne 1979; (5) Peacock et al. 1981 [0404 + 768, 0814 + 425, 1031 + 567]; (6) H. Spinrad 1986, private communication [1157 + 732]; (7) Spinrad 1982 [1254 + 476]; (8) Bartel et al. 1984b [2021 + 641].

Col. (11).—"Y" if the source was detected in the VLBI finding survey, "N" if it was not.

Col. (12).—Date of first-epoch mapping observation.

Col. (13).—Antennas used in map (for abbreviations see notes to Table 2).

Col. (14).—Total 5 GHz flux density (Jy) of the source in the published survey (S4 or S5).

Col. (15).—Total 5 GHz flux density (Jy) of the source at the time of the VLBI observation.

Col. (16).—Fraction F_c of the total flux density in an unresolved core (see § V).

Col. (17).—Morphological class (see § V).

TABLE 2

JOURNAL OF OBSERVATIONS

Source	Epoch	Antennasa	Frequency (MHz)	Integration Time	Polarization ^b	Total Tim Scheduled (hr)
Source	Epoch	Antennas	· · · · · · · · · · · · · · · · · · ·	(s)	Folarization	(111)
			1978 Dec 11–14			
0133 + 476	1978.95	GFOH	5011	120	Lin 90	5
0316 + 413	1978.95	GFOH	5011	120	Lin 90	10.5
$0859 + 470 \dots$	1978.95	GFOH	5011	120	Lin 90	9.5
$0923 + 392 \dots$	1978.95	GFOH	5011	120	Lin 90	11.5
1633 + 382	1978.95	GFOH	5011	120	Lin 90	2
1807 + 698	1978.95	GFOH	5011	120	Lin 90	8.5
1828 + 487	1978.95	GFOH	5011	120	Lin 90	9.5
2200 + 420	1978.95	GFOH	5011	120	Lin 90	10
			1979 Apr 1°		1	
1633 + 382	1979.25	BGFOH	4996	120	Lin 90	6.5
			1979 Jul 24-26			
0108 + 388	1979.56	GFOH	5011	60	Lin 90	12
0814 + 425	1979.56	GFOH	5011	60	Lin 90	13
945 + 408	1979.56	GFOH	5011	60	Lin 90	12.5
637 + 574	1979.56	GFOH	5011	60	Lin 90	12.5
1823 + 568	1979.56	GFOH	5011	60	Lin 90	3
954 + 513	1979.56	GFOH	5011	60	Lin 90	11.5
		19	979 Nov 30–Dec	2 ^d		
0804 + 499	1979.92	BKGFO	5009	240	Lin 90	11
0831 + 557	1979.91	KGFO	5009	240	Lin 90	11
906 + 430	1979.92	BKGFO	5009	240	Lin 90	8
358 + 624	1979.92	BG	5009	240	Lin 90	ğ
823 + 568	1979.92	BKGFO	5009	240	Lin 90	10.5
2021 + 614	1979.92	KGFO	5009	240	Lin 90 Lin 90	10.3
2352 + 495	1979.91	BKGFO	5009	240	Lin 90	10
	· · · · · · · · · · · · · · · · · · ·	· · · · · · · · · · · · · · · · · · ·	1980 Jul 11-14			
0710+439	1980.53	BKGFO	5011	120	LCP	11
0711 + 356	1980.53	BKGFO	5011	120	LCP	10
0850 + 581	1980.53	BKFO	5011	120	LCP	11.5
624 + 413	1980.53	BKGFO	5011	120	LCP	9.5
642 + 690	1980.53	BKGFO	5011	120	LCP	12
652 + 398	1980.53	BKGFO	5011	120	LCP	10
2351 + 456	1980.53	BKGFO	5011	120	LCP	5
			1980 Sep 19-26e			
016+731	1980.74	BKFO	5009	120	LCP	1
153 + 744	1980.74	BKFO	5009	120	LCP	1
212 + 735	1980.72	BKFO	5009	120	LCP	9
404 + 768	1980.74	B(KF)O	5009	120	LCP	1
454 + 844	1980.73	BKFO	5009	120	LCP	8.5
538 + 498	1980.74	(K)FO	5009	120	LCP	1
836 + 710	1980.72	BKFO	5009	120	LCP	6.5
$749 + 701 \dots$	1980.74	BKFO	5009	120	LCP	0.5
803 + 784	1980.74	BKFO	5009	120	LCP	0.5
928 + 738	1980.72	BKFO	5009	120	LCP	9
342 + 821	1980.74	(BKFO)	5009	120	LCP	1
		1	1981 Aug 22-23	× X		
0454 + 844	1981.64	BKGFO	4989	120	LCP	11
458 + 718	1981.64	BKGFO	4989	120	LCP	11
			1982 Apr 1-5	-		
0016 + 731	1982.25	BKGFO	4989	120	LCP	14
$0153 + 744 \dots$	1982.26	BGFO	4989	120	LCP	11
$739 + 522 \dots$	1982.26	BGFO	4989	120	LCP	9
749 + 701	1982.26	BKGFO	4989	120	LCP	6
803 + 784	1982.26	BKGFO	4989	120	LCP	6

PEARSON AND READHEAD

TABLE 3
Map Parameters

01084 388.				ВЕА	M ^a		
01084 388.	Source	OBSERVATION	а	b	•		
0133 + 476	0016 + 731						± 0.5 , ± 1 , 2, 5, 10, 20, 30, 40, 50, 60, 70, 80, 90
0153+744.						0.99	± 1 , 3, 5, 7, 10, 15, 20, 30, 40, 50, 60, 70, 80, 90
0212+735.							± 1 , 2, 3, 4, 5, 10, 20, 30, 40, 50, 60, 70, 80, 90
0316+413 1978 Dec 2.8 2.2 11 15.50 ±2.5, 5, 7.5, 10, 20, 30, 40, 50, 60, 70, 80, 90 0454+844 1981 Aug 1.3 1.3 0 0.72 ±2, 5, 10, 20, 30, 40, 50, 60, 70, 80, 90 0710+439 1980 Jul 1.4 1.0 -25 0.32 ±2, ±5, 10, 20, 30, 40, 50, 60, 70, 80, 90 0804+499 1979 Dec 1.3 1.0 90 1.29 ±0.25, ±0.5, 1, 2, 3, 4, 5, 10, 20, 30, 40, 50, 60, 70, 80, 90 0814+425 1979 Jul 3.2 2.1 23 1.49 ±1, ±3, 6, 10, 20, 30, 40, 50, 60, 70, 80, 90 0836+710 1980 Sul 1.5 0.8 -63 0.68 ±2, ±5, 10, 20, 30, 40, 50, 60, 70, 80, 90 0836+710 1980 Sep 1.3 1.0 90 0.88 ±2, 4, 6, 8, 10, 20, 30, 40, 50, 60, 70, 80, 90 0850+581 1980 Jul 1.5 0.8 -63 0.68 ±2, ±5, 10, 20, 30, 40, 50, 60, 70, 80, 90 0859+581 1980 Jul 1.5 0.8 -63 0.68 ±2, ±5, 10, 20, 30, 40, 50, 60, 70, 80, 90 0906+430 1979 Dec 2.9 2.1 11 0.85 ±1, 2, 3, 4, 5, 10, 20, 30, 40, 50, 60, 70, 80, 90 0923+392 1978 Dec 3.0 2.2 15 4.28 ±1, 2, 3, 4, 5, 10, 20, 30, 40, 50, 60, 70, 80, 90 0945+408 1979 Jul 2.9 2.1 11 0.70 ±1, ±3, 5, 7, 10, 15, 20, 30, 40, 50, 60, 70, 80, 90 1458+718 1981 Aug 1.3 1.3 0 0.31 ±2, ±5, 10, 20, 30, 40, 50, 60, 70, 80, 90 1624+416 1980 Jul 1.8 0.8 -63 0.41 ±2, ±5, 10, 20, 30, 40, 50, 60, 70, 80, 90 1637+574 1979 Jul 2.7 2.1 31 1.65 ±1, ±3, 5, 7, 10, 15, 20, 30, 40, 50, 60, 70, 80, 90 1637+574 1979 Jul 2.7 2.1 31 1.65 ±1, ±3, 5, 10, 20, 30, 40, 50, 60, 70, 80, 90 1637+574 1979 Jul 2.7 2.1 31 1.65 ±1, ±3, 5, 10, 20, 30, 40, 50, 60, 70, 80, 90 1637+574 1979 Jul 2.7 2.1 31 1.65 ±1, ±3, 5, 10, 20, 30, 40, 50, 60, 70, 80, 90 1637+574 1979 Jul 2.7 2.1 31 1.65 ±1, ±3, 5, 10, 20, 30, 40, 50, 60, 70, 80, 90 1652+398 1980 Jul 1.9 0.9 -26 0.53 ±0.5, 1, ±2, 5, 10, 20, 30, 40, 50, 60, 70, 80, 90 1803+784 1980 Jul 1.9 0.9 -26 0.53 ±0.5, 1, ±2, 5, 10, 20, 30, 40, 50, 60, 70, 80, 90 1803+784 1980 Jul 1.9 0.9 -26 0.53 ±0.5, 1, ±2, 5, 10, 20, 30, 40, 50, 60, 70, 80, 90 1803+831 1979 Dec 2.9 2.1 10 1.01 ±2.5, 5, 7.5, 10, 20, 30, 40, 50, 60, 70, 80, 90 1803+831 1979 Dec 2.9 2.1 10 1.01 ±2.5, 5, 7.5, 10, 20, 30, 40, 50, 60							
0454 + 844.	0212 + 735	1980 Sep	1.3	1.0	110	1.14	± 1 , ± 2 , 3, 4, 6, 8, 10, 20, 30, 40, 50, 60, 70, 80, 90
0710+439.	0316+413	1978 Dec	2.8	2.2	11	15.50	± 2.5 , 5, 7.5, 10, 20, 30, 40, 50, 60, 70, 80, 90
0710+439	$0454 + 844 \dots$	1981 Aug	1.3	1.3	0	0.72	
0711+356	$0710 + 439 \dots$	1980 Jul	1.4	1.0	-25	0.32	
0804 + 499	0711 + 356	1980 Jul	1.8	0.8	-24	0.48	
0831+557. 1979 Dec 2.0 2.0 0 0.77 ±1, ±2, 3, 4, 5, 10, 20, 30, 40, 50, 60, 70, 80, 90 0836+710. 1980 Sep 1.3 1.0 90 0.88 ±2, 4, 6, 8, 10, 20, 30, 40, 50, 60, 70, 80, 90 0859+870. 1978 Dec 2.9 2.1 11 0.85 ±1, ±2, 3, 4, 5, 10, 20, 30, 40, 50, 60, 70, 80, 90 0906+430. 1979 Dec 1.5 1.0 145 0.87 ±0.5, ±1, 2, 3, 4, 5, 10, 20, 30, 40, 50, 60, 70, 80, 90 0923+392. 1978 Dec 3.0 2.2 15 428 ±1, 2, 3, 4, 5, 10, 20, 30, 40, 50, 60, 70, 80, 90 0945+408. 1979 Jul 2.9 2.1 11 0.70 ±1, ±3, 5, 7, 10, 15, 20, 30, 40, 50, 60, 70, 80, 90 1458+718. 1981 Aug 1.3 1.3 0 0.31 ±2, ±5, 10, 20, 30, 40, 50, 60, 70, 80, 90 1624+416. 1980 Jul 1.8 0.8 -63 0.41 ±2, ±5, 10, 20, 30, 40, 50, 60, 70, 80, 90 1633+382. 1979 Apr 1.8 1.0 -24 1.21 ±0.5, 1, 2, 3, 4, 5, 10, 20, 30, 40, 50, 60, 70, 80, 90 1642+690. 1980 Jul 1.2 1.1 0 1.39 ±0.4 ±1.2, 5, 10, 20, 30, 40, 50, 60, 70, 80, 90 1652+398. 1980 Jul 1.2 1.1 0 1.39 ±0.4 ±1.2, 5, 10, 20, 30, 40, 50, 60, 70, 80, 90 1652+398. 1980 Jul 1.9 0.9 -26 0.53 ±0.5, ±1, ±2, 5, 10, 20, 30, 40, 50, 60, 70, 80, 90 1652+398. 1980 Jul 1.9 0.9 -26 0.53 ±0.5, ±1, ±2, 5, 10, 20, 30, 40, 50, 60, 70, 80, 90 1739+522. 1982 Apr 1.1 1.1 0 0.82 ±1, 2, 5, 10, 20, 30, 40, 50, 60, 70, 80, 90 1749+701. 1982 Apr 1.1 1.1 0 0.82 ±1, 2, 5, 10, 20, 30, 40, 50, 60, 70, 80, 90 1807+698. 1978 Dec 2.8 1.7 -10 0.92 ±2.5, 5, 7.5, 10, 20, 30, 40, 50, 60, 70, 80, 90 1823+568. 1979 Dec 1.1 1.1 0 0.082 ±1, 2, 5, 10, 20, 30, 40, 50, 60, 70, 80, 90 1828+568. 1979 Dec 1.1 1.1 0 0.082 ±1, 2, 5, 10, 20, 30, 40, 50, 60, 70, 80, 90 1828+568. 1978 Dec 2.9 2.1 10 1.01 ±2.5, 5, 7.5, 10, 20, 30, 40, 50, 60, 70, 80, 90 1828+788. 1980 Sep 1.3 1.0 140 1.46 ±1, 2, 3, 4, 5, 10, 20, 30, 40, 50, 60, 70, 80, 90 1828+788. 1980 Sep 1.3 1.0 140 1.46 ±1, 2, 3, 4, 5, 10, 20, 30, 40, 50, 60, 70, 80, 90 1928+738. 1980 Sep 1.3 1.0 140 1.46 ±1, 2, 3, 4, 5, 10, 20, 30, 40, 50, 60, 70, 80, 90 1928+738. 1990 Dec 2.0 0 0.90 ±2.4, 6, 8, 10, 20, 30, 40, 50, 60, 70, 80, 90 1928+738. 1990 Dec 2.0 2.0 0 0.90 ±2.4, 6, 8, 10, 20, 30, 40, 50, 60, 70, 80, 90 1928+738. 1990 Dec 2.0 2.0 0	0804 + 499	1979 Dec	1.3	1.0	90	1.29	$\pm 0.25, \pm 0.5, 1, 2, 3, 4, 5, 10, 20, 30, 40, 50, 60, 70, 80, 90$
0831 + 557. 1979 Dec 2.0 2.0 0 0 0.777	0814+425	1979 Jul	3.2	2.1	23	1 49	+1 +3 6 10 20 30 40 50 60 70 80 90
0836 + 710.	$0831 + 557 \dots$	1979 Dec	2.0	2.0			
0859 + 581	$0836 + 710 \dots$	1980 Sep	1.3	1.0			
0859 + 470. 1978 Dec 2.9 2.1 11 0.85 ±1, 2, 3, 4, 5, 10, 20, 30, 40, 50, 60, 70, 80, 90 0906 + 430. 1979 Dec 1.5 1.0 145 0.87 ±0.5, ±1, 2, 3, 4, 5, 10, 20, 30, 40, 50, 60, 70, 80, 90 0923 + 392. 1978 Dec 3.0 2.2 15 4.28 ±1, 2, 3, 4, 5, 10, 20, 30, 40, 50, 60, 70, 80, 90 0945 + 408. 1979 Jul 2.9 2.1 11 0.70 ±1, ±3, 5, 7, 10, 15, 20, 30, 40, 50, 60, 70, 80, 90 1458 + 718. 1981 Aug 1.3 1.3 0 0.31 ±2, ±5, 10, 20, 30, 40, 50, 60, 70, 80, 90 1624 + 416. 1980 Jul 1.8 0.8 -63 0.41 ±2, ±5, 10, 20, 30, 40, 50, 60, 70, 80, 90 1637 + 574 1979 Jul 2.7 2.1 31 1.65 ±1, ±3, 5, 10, 20, 30, 40, 50, 60, 70, 80, 90 1637 + 574 1979 Jul 2.7 2.1 31 1.65 ±1, ±3, 6, 10, 20, 30, 40, 50, 60, 70, 80, 90 1652 + 398. 1980 Jul 1.9 0.9 -26 0.53 ±0.5, ±1, ±2, 5, 10, 20, 30, 40, 50, 60, 70, 80, 90 1739 + 522. 1982 Apr 1.1 0.8 -45 0.80 ±0.5, ±1, ±2, 5, 10, 20, 30, 40, 50, 60, 70, 80, 90 1749 + 701 1982 Apr 1.1 1.1 0 0.82 ±1, 2, 5, 10, 20, 30, 40, 50, 60, 70, 80, 90 1803 + 784 1982 Apr 1.1 1.1 0 0.82 ±1, 2, 5, 10, 20, 30, 40, 50, 60, 70, 80, 90 1823 + 868. 1979 Dec 2.8 1.7 -10 0.92 ±2.5, 5, 7.5, 10, 20, 30, 40, 50, 60, 70, 80, 90 1823 + 487 1978 Dec 2.9 2.1 10 1.01 ±2.5, 5, 7.5, 10, 20, 30, 40, 50, 60, 70, 80, 90 1828 + 487 1978 Dec 2.9 2.1 10 1.01 ±2.5, 5, 7.5, 10, 20, 30, 40, 50, 60, 70, 80, 90 1828 + 487 1982 Apr 1.8 1.5 90 0.27 ±2.5, 5, 7.5, 10, 20, 30, 40, 50, 60, 70, 80, 90 1828 + 487 1982 Apr 1.8 1.5 90 0.27 ±2.5, 5, 7.5, 10, 20, 30, 40, 50, 60, 70, 80, 90 1828 + 487 1982 Apr 1.8 1.5 90 0.27 ±2.5, 5, 7.5, 10, 20, 30, 40, 50, 60, 70, 80, 90 1828 + 487 1982 Apr 1.8 1.5 90 0.27 ±2.5, 5, 7.5, 10, 20, 30, 40, 50, 60, 70, 80, 90 1828 + 487 1998 Dec 2.9 2.1 10 1.01 ±2.5, 5, 7.5, 10, 20, 30, 40, 50, 60, 70, 80, 90 1928 + 738 1980 Sep 1.3 1.0 140 1.46 ±1, 2, 3, 4, 6, 8, 10, 20, 30, 40, 50, 60, 70, 80, 90 1928 + 738 1980 Sep 1.3 1.0 140 1.46 ±1, 2, 3, 4, 6, 8, 10, 20, 30, 40, 50, 60, 70, 80, 90 1924 + 738 1980 Sep 1.3 1.0 140 1.46 ±1, 2, 3, 4, 6, 8, 10, 20, 30, 40, 50, 60, 70, 80, 90 1924 + 746 11 1979 Dec 2.0 2.0 0 0.90 ±2, 4, 6, 8, 10, 20, 30, 40,	$0850 + 581 \dots$						
0906 + 430 1979 Dec 1.5 1.0 145 0.87 ±0.5, ±1, 2, 3, 4, 5, 10, 20, 30, 40, 50, 60, 70, 80, 90 0923 + 392 1978 Dec 3.0 2.2 15 4.28 ±1, 2, 3, 4, 5, 10, 20, 30, 40, 50, 60, 70, 80, 90 0945 + 408 1979 Jul 2.9 2.1 11 0.70 ±1, ±3, 5, 7, 10, 15, 20, 30, 40, 50, 60, 70, 80, 90 09.0 1458 + 718 1981 Aug 1.3 1.3 0 0.31 ±2, ±5, 10, 20, 30, 40, 50, 60, 70, 80, 90 1624 + 416 1980 Jul 1.8 0.8 -63 0.41 ±2, ±5, 10, 20, 30, 40, 50, 60, 70, 80, 90 1633 + 382 1979 Apr 1.8 1.0 -24 1.21 ±0.5, 1, 2, 3, 4, 5, 10, 20, 30, 40, 50, 60, 70, 80, 90 1637 + 574 1979 Jul 2.7 2.1 31 1.65 ±1, ±3, 6, 10, 20, 30, 40, 50, 60, 70, 80, 90 1642 + 690 1980 Jul 1.2 1.1 0 1.39 ±0.4, ±1.2, 2, 5, 10, 20, 30, 40, 50, 60, 70, 80, 90 1652 + 398 1980 Jul 1.9 0.9 -26 0.53 ±0.5, ±1, ±2, 5, 10, 20, 30, 40, 50, 60, 70, 80, 90 1679 + 522 1982 Apr 1.1 0.8 -45 0.80 ±0.5, ±2, 5, 10, 20, 30, 40, 50, 60, 70, 80, 90 1803 + 784 1982 Apr 1.1 1.1	$0859 + 470 \dots$						
0923 + 392 1978 Dec 3.0 2.2 15 4.28 ±1, 2, 3, 4, 5, 10, 20, 30, 40, 50, 60, 70, 80, 90 0945 + 408 1979 Jul 2.9 2.1 11 0.70 ±1, ±3, 5, 7, 10, 15, 20, 30, 40, 50, 60, 70, 80, 90 1458 + 718 1981 Aug 1.3 1.3 0 0.31 ±2, ±5, 10, 20, 30, 40, 50, 60, 70, 80, 90 1624 + 416 1980 Jul 1.8 0.8 -63 0.41 ±2, ±5, 10, 20, 30, 40, 50, 60, 70, 80, 90 1633 + 382 1979 Apr 1.8 1.0 -24 1.21 ±0.5, 1, 2, 3, 4, 5, 10, 20, 30, 40, 50, 60, 70, 80, 90 1637 + 574 1979 Jul 2.7 2.1 31 1.65 ±1, ±3, 6, 10, 20, 30, 40, 50, 60, 70, 80, 90 1642 + 690 1980 Jul 1.2 1.1 0 1.39 ±0.4, ±1.2, 2, 5, 10, 20, 30, 40, 50, 60, 70, 80, 90 1652 + 398 1980 Jul 1.9 0.9 -26 0.53 ±0.5, ±1, ±2, 5, 10, 20, 30, 40, 50, 60, 70, 80, 90 1739 + 522 1982 Apr 1.1 0.8 -45 0.80 ±0.5, 1, 2, 5, 10, 20, 30, 40, 50, 60, 70, 80, 90 1803 + 84 1982 Apr 1.1 1.1 0 0.82 ±1, 2, 5, 10, 20, 30, 40, 50, 60, 70, 80, 90 1803 + 84 1982 Apr 1.1 1.1 0 0.82 ±1, 2, 5, 10, 20, 30, 40, 50, 60, 70, 80, 90 1807 + 698 1978 Dec 2.8 1.7 -10 0.92 ±2.5, 5, 7.5, 10, 20, 30, 40, 50, 60, 70, 80, 90 1823 + 568 1979 Dec 1.1 1.1 0 1.08 ±0.5, ±1, 2, 3, 4, 5, 10, 20, 30, 40, 50, 60, 70, 80, 90 1824 + 487 1978 Dec 2.9 2.1 10 1.01 ±2.5, 5, 7.5, 10, 20, 30, 40, 50, 60, 70, 80, 90 1828 + 487 1978 Dec 2.9 2.1 10 1.01 ±2.5, 5, 7.5, 10, 20, 30, 40, 50, 60, 70, 80, 90 1828 + 788 1980 Sep 1.3 1.0 140 1.46 ±1, 2, 3, 4, 5, 10, 20, 30, 40, 50, 60, 70, 80, 90 1928 + 738 1980 Sep 1.3 1.0 140 1.46 ±1, 2, 3, 4, 5, 10, 20, 30, 40, 50, 60, 70, 80, 90 2021 + 614 1979 Dec 2.0 2.0 0 0.90 ±2, 4, 6, 8, 10, 20, 30, 40, 50, 60, 70, 80, 90 2200 + 420 1978 Dec 2.9 2.4 11 1.20 ±1, ±2, ±3, 4, 5, 10, 20, 30, 40, 50, 60, 70, 80, 90 2200 + 420 1978 Dec 2.9 2.4 11 1.20 ±1, ±2, ±3, 4, 5, 10, 20, 30, 40, 50, 60, 70, 80, 90 2201 + 614 1979 Dec 2.0 2.0 0 0.90 ±2, 4, 6, 8, 10, 20, 30, 40, 50, 60, 70, 80, 90 2201 + 614 1979 Dec 2.0 2.0 0 0.90 ±2, 4, 6, 8, 10, 20, 30, 40, 50, 60, 70, 80, 90 2201 + 614 1979 Dec 2.0 5.0 0 0.90 ±2, 4, 6, 8, 10, 20, 30, 40, 50, 60, 70, 80, 90 2201 + 614	0906 + 430	1979 Dec	1.5	1.0	145	0.87	
0945 + 408 1979 Jul 2.9 2.1 11 0.70 ±1, ±3, 5, 7, 10, 15, 20, 30, 40, 50, 60, 70, 80, 90 1458 + 718 1981 Aug 1.3 1.3 0 0.31 ±2, ±5, 10, 20, 30, 40, 50, 60, 70, 80, 90 1624 + 416 1980 Jul 1.8 0.8 -63 0.41 ±2, ±5, 10, 20, 30, 40, 50, 60, 70, 80, 90 1633 + 382 1979 Apr 1.8 1.0 -24 1.21 ±0.5, 1, 2, 3, 4, 5, 10, 20, 30, 40, 50, 60, 70, 80, 90 1637 + 574 1979 Jul 2.7 2.1 31 1.65 ±1, ±3, 6, 10, 20, 30, 40, 50, 60, 70, 80, 90 1632 + 690 1980 Jul 1.2 1.1 0 1.39 ±0.4, ±1.2, 2, 5, 10, 20, 30, 40, 50, 60, 70, 80, 90 1652 + 398 1980 Jul 1.9 0.9 -26 0.53 ±0.5, ±1, ±2, 5, 10, 20, 30, 40, 50, 60, 70, 80, 90 1739 + 522 1982 Apr 1.1 0.8 -45 0.80 ±0.5, ±2, 5, 10, 20, 30, 40, 50, 60, 70, 80, 90 1749 + 701 1982 Apr 1.1 1.1 0 0.82 ±1, 2, 5, 10, 20, 30, 40, 50, 60, 70, 80, 90 1803 + 784 1982 Apr 1.1 1.1 0 0.217 ±1, 2, 5,	$0923 + 392 \dots$						
1458 + 718 1981 Aug 1.3 1.3 0 0.31 ±2, ±5, 10, 20, 30, 40, 50, 60, 70, 80, 90 1624 + 416 1980 Jul 1.8 0.8 -63 0.41 ±2, ±5, 10, 20, 30, 40, 50, 60, 70, 80, 90 1633 + 382 1979 Apr 1.8 1.0 -24 1.21 ±0.5, 1, 2, 3, 4, 5, 10, 20, 30, 40, 50, 60, 70, 80, 90 1637 + 574 1979 Jul 2.7 2.1 31 1.65 ±1, ±3, 6, 10, 20, 30, 40, 50, 60, 70, 80, 90 1642 + 690 1980 Jul 1.2 1.1 0 1.39 ±0.4, ±1.2, 2, 5, 10, 20, 30, 40, 50, 60, 70, 80, 90 1739 + 522 1982 Apr 1.1 0.8 -45 0.80 ±0.5, ±1, ±2, 5, 10, 20, 30, 40, 50, 60, 70, 80, 90 1749 + 701 1982 Apr 1.1 1.1 0 0.82 ±1, 2, 5, 10, 20, 30, 40, 50, 60, 70, 80, 90 1803 + 784 1982 Apr 1.1 1.1 0 0.82 ±1, 2, 5, 10, 20, 30, 40, 50, 60, 70, 80, 90 1823 + 568 1979 Dec 1.1 1.1 0 0.217 ±1, 2, 5, 10, 20, 30, 40, 50, 60, 70, 80, 90 1828 + 487 1982 Apr 1.8 1.5 90 0.27 ±2, 5, 7, 5, 10, 20, 3	0945 + 408						
1624+416. 1980 Jul 1.8 0.8 -63 0.41 ±2, ±5, 10, 20, 30, 40, 50, 60, 70, 80, 90 1633+382. 1979 Apr 1.8 1.0 -24 1.21 ±0.5, 1, 2, 3, 4, 5, 10, 20, 30, 40, 50, 60, 70, 80, 90 1637+574. 1979 Jul 2.7 2.1 31 1.65 ±1, ±3, 6, 10, 20, 30, 40, 50, 60, 70, 80, 90 1642+690. 1980 Jul 1.2 1.1 0 1.39 ±0.4, ±1.2, 2, 5, 10, 20, 30, 40, 50, 60, 70, 80, 90 1652+398. 1980 Jul 1.9 0.9 -26 0.53 ±0.5, ±1, ±2, 5, 10, 20, 30, 40, 50, 60, 70, 80, 90 1739+522. 1982 Apr 1.1 0.8 -45 0.80 ±0.5, ±2, 5, 10, 20, 30, 40, 50, 60, 70, 80, 90 1749+701. 1982 Apr 1.1 1.1 0 0.82 ±1, 2, 5, 10, 20, 30, 40, 50, 60, 70, 80, 90 1807+698. 1982 Apr 1.1 1.1 0 2.17 ±1, 2, 5, 10, 20, 30, 40, 50, 60, 70, 80, 90 1823+568. 1979 Dec 2.8 1.7 -10 0.92 ±2.5, 5, 7.5, 10, 20, 30, 40, 50, 60, 70, 80, 90 1828+487. 1978 Dec 2.9 2.1 10 1.01 ±2.5, 5, 7.5, 10, 20	1458 + 718						
$\begin{array}{cccccccccccccccccccccccccccccccccccc$	1624+416						
1637 + 574 1979 Jul 2.7 2.1 31 1.65 ±1, ±3, 6, 10, 20, 30, 40, 50, 60, 70, 80, 90 1642 + 690 1980 Jul 1.2 1.1 0 1.39 ±0.4, ±1.2, 2, 5, 10, 20, 30, 40, 50, 60, 70, 80, 90 1652 + 398 1980 Jul 1.9 0.9 -26 0.53 ±0.5, ±1, ±2, 5, 10, 20, 30, 40, 50, 60, 70, 80, 90 1739 + 522 1982 Apr 1.1 0.8 -45 0.80 ±0.5, 1, 2, 5, 10, 20, 30, 40, 50, 60, 70, 80, 90 1749 + 701 1982 Apr 1.1 1.1 0 0.82 ±1, 2, 5, 10, 20, 30, 40, 50, 60, 70, 80, 90 1803 + 784 1982 Apr 1.1 1.1 0 2.17 ±1, 2, 5, 10, 20, 30, 40, 50, 60, 70, 80, 90 1807 + 698 1978 Dec 2.8 1.7 -10 0.92 ±2.5, 5, 7.5, 10, 20, 30, 40, 50, 60, 70, 80, 90 1823 + 568 1979 Dec 1.1 1.1 0 1.08 ±0.5, ±1, 2, 3, 4, 5, 10, 20, 30, 40, 50, 60, 70, 80, 90 1828 + 487 1978 Dec 2.9 2.1 10 1.01 ±2.5, 5, 7.5, 10, 20, 30, 40, 50, 60, 70, 80, 90 1845 + 797 1982 Apr 1.8 1.5 90 0.27 ±2,	1633 + 382	1979 Apr	1.8	1.0	-24	1 21	+0.5 1 2 3 4 5 10 20 30 40 50 60 70 80 90
$ \begin{array}{cccccccccccccccccccccccccccccccccccc$	1637 + 574						
1652+398 1980 Jul 1.9 0.9 -26 0.53 ±0.5, ±1, ±2, 5, 10, 20, 30, 40, 50, 60, 70, 80, 90 1739+522 1982 Apr 1.1 0.8 -45 0.80 ±0.5, 1, 2, 5, 10, 20, 30, 40, 50, 60, 70, 80, 90 1749+701 1982 Apr 1.1 1.1 0 0.82 ±1, 2, 5, 10, 20, 30, 40, 50, 60, 70, 80, 90 1803+784 1982 Apr 1.1 1.1 0 2.17 ±1, 2, 5, 10, 20, 30, 40, 50, 60, 70, 80, 90 1807+698 1978 Dec 2.8 1.7 -10 0.92 ±2.5, 5, 7.5, 10, 20, 30, 40, 50, 60, 70, 80, 90 1823+568 1979 Dec 1.1 1.1 0 1.08 ±0.5, ±1, 2, 3, 4, 5, 10, 20, 30, 40, 50, 60, 70, 80, 90 1828+487 1978 Dec 2.9 2.1 10 1.01 ±2.5, 5, 7.5, 10, 20, 30, 40, 50, 60, 70, 80, 90 1845+797 1982 Apr 1.8 1.5 90 0.27 ±2, 5, 10, 20, 30, 40, 50, 60, 70, 80, 90 1928+738 1980 Sep 1.3 1.0 140 1.46 ±1, 2, 3, 4, 6, 8, 10, 20, 30, 40, 50, 60, 70, 80, 90 2021+614 1979 Dec 2.0 -19 0.71 ±2, 6, 10, 20		1980 Jul					
1739 + 522 1982 Apr 1.1 0.8 -45 0.80 ±0.5, 1, 2, 5, 10, 20, 30, 40, 50, 60, 70, 80, 90 1749 + 701 1982 Apr 1.1 1.1 0 0.82 ±1, 2, 5, 10, 20, 30, 40, 50, 60, 70, 80, 90 1803 + 784 1982 Apr 1.1 1.1 0 2.17 ±1, 2, 5, 10, 20, 30, 40, 50, 60, 70, 80, 90 1807 + 698 1978 Dec 2.8 1.7 -10 0.92 ±2.5, 5, 75, 10, 20, 30, 40, 50, 60, 70, 80, 90 1823 + 568 1979 Dec 1.1 1.1 0 1.08 ±0.5, ±1, 2, 3, 4, 5, 10, 20, 30, 40, 50, 60, 70, 80, 90 1828 + 487 1978 Dec 2.9 2.1 10 1.01 ±2.5, 5, 7.5, 10, 20, 30, 40, 50, 60, 70, 80, 90 1845 + 797 1982 Apr 1.8 1.5 90 0.27 ±2, 5, 10, 20, 30, 40, 50, 60, 70, 80, 90 1928 + 738 1980 Sep 1.3 1.0 140 1.46 ±1, 2, 3, 4, 6, 8, 10, 20, 30, 40, 50, 60, 70, 80, 90 1954 + 513 1979 Jul 2.9 2.0 -19 0.71 ±2, 6, 10, 20, 30, 40, 50, 60, 70, 80, 90 2021 + 614 1979 Dec 2.0 2.0 0 0.90 ±2, 4, 6, 8, 10,	1652 + 398						
1749 + 701 1982 Apr 1.1 1.1 0 0.82 ±1, 2, 5, 10, 20, 30, 40, 50, 60, 70, 80, 90 1803 + 784 1982 Apr 1.1 1.1 0 2.17 ±1, 2, 5, 10, 20, 30, 40, 50, 60, 70, 80, 90 1807 + 698 1978 Dec 2.8 1.7 -10 0.92 ±2.5, 5, 75, 10, 20, 30, 40, 50, 60, 70, 80, 90 1823 + 568 1979 Dec 1.1 1.1 0 1.08 ±0.5, ±1, 2, 3, 4, 5, 10, 20, 30, 40, 50, 60, 70, 80, 90 1828 + 487 1978 Dec 2.9 2.1 10 1.01 ±2.5, 5, 7.5, 10, 20, 30, 40, 50, 60, 70, 80, 90 1845 + 797 1982 Apr 1.8 1.5 90 0.27 ±2, 5, 10, 20, 30, 40, 50, 60, 70, 80, 90 1928 + 738 1980 Sep 1.3 1.0 140 1.46 ±1, 2, 3, 4, 6, 8, 10, 20, 30, 40, 50, 60, 70, 80, 90 1954 + 513 1979 Jul 2.9 2.0 -19 0.71 ±2, 6, 10, 20, 30, 40, 50, 60, 70, 80, 90 2021 + 614 1979 Dec 2.0 2.0 0 0.90 ±2, 4, 6, 8, 10, 20, 30, 40, 50, 60, 70, 80, 90 2230 + 420 1978 Dec 2.9 2.4 11 1.20 ±1, ±2, ±3, 4, 5, 10	$1739 + 522 \dots$	1982 Apr					
1803 + 784 1982 Apr 1.1 1.1 0 2.17 ±1, 2, 5, 10, 20, 30, 40, 50, 60, 70, 80, 90 1807 + 698 1978 Dec 2.8 1.7 -10 0.92 ±2.5, 5, 7.5, 10, 20, 30, 40, 50, 60, 70, 80, 90 1823 + 568 1979 Dec 1.1 1.1 0 1.08 ±0.5, ±1, 2, 3, 4, 5, 10, 20, 30, 40, 50, 60, 70, 80, 90 1828 + 487 1978 Dec 2.9 2.1 10 1.01 ±2.5, 5, 7.5, 10, 20, 30, 40, 50, 60, 70, 80, 90 1845 + 797 1982 Apr 1.8 1.5 90 0.27 ±2, 5, 10, 20, 30, 40, 50, 60, 70, 80, 90 1928 + 738 1980 Sep 1.3 1.0 140 1.46 ±1, 2, 3, 4, 6, 8, 10, 20, 30, 40, 50, 60, 70, 80, 90 1954 + 513 1979 Jul 2.9 2.0 -19 0.71 ±2, 6, 10, 20, 30, 40, 50, 60, 70, 80, 90 2021 + 614 1979 Dec 2.0 2.0 0 0.90 ±2, 4, 6, 8, 10, 20, 30, 40, 50, 60, 70, 80, 90 2200 + 420 1978 Dec 2.9 2.4 11 1.20 ±1, ±2, ±3, 4, 5, 10, 20, 30, 40, 50, 60, 70, 80, 90 2351 + 456 1980 Jul 3.8 0.9 -15 0.27 ±5, 15, 2	1749 + 701	1982 Apr	1.1	11	0	0.82	
1807 + 698 1978 Dec 2.8 1.7 -10 0.92 ±2.5, 5, 7.5, 10, 20, 30, 40, 50, 60, 70, 80, 90 1823 + 568 1979 Dec 1.1 1.1 0 1.08 ±0.5, ±1, 2, 3, 4, 5, 10, 20, 30, 40, 50, 60, 70, 80, 90 1828 + 487 1978 Dec 2.9 2.1 10 1.01 ±2.5, 5, 7.5, 10, 20, 30, 40, 50, 60, 70, 80, 90 1845 + 797 1982 Apr 1.8 1.5 90 0.27 ±2, 5, 10, 20, 30, 40, 50, 60, 70, 80, 90 1928 + 738 1980 Sep 1.3 1.0 140 1.46 ±1, 2, 3, 4, 6, 8, 10, 20, 30, 40, 50, 60, 70, 80, 90 1954 + 513 1979 Jul 2.9 2.0 -19 0.71 ±2, 6, 10, 20, 30, 40, 50, 60, 70, 80, 90 2021 + 614 1979 Dec 2.0 2.0 0 0.90 ±2, 4, 6, 8, 10, 20, 30, 40, 50, 60, 70, 80, 90 2200 + 420 1978 Dec 2.9 2.4 11 1.20 ±1, ±2, ±3, 4, 5, 10, 20, 30, 40, 50, 60, 70, 80, 90 2351 + 456 1980 Jul 3.8 0.9 -15 0.27 ±5, 15, 25, 35, 45, 55, 65, 75, 85, 95	1803 + 784						
1823 + 568. 1979 Dec 1.1 1.1 0 1.08 ±0.5, ±1, 2, 3, 4, 5, 10, 20, 30, 40, 50, 60, 70, 80, 90 1828 + 487. 1978 Dec 2.9 2.1 10 1.01 ±2.5, 5, 7.5, 10, 20, 30, 40, 50, 60, 70, 80, 90 1845 + 797. 1982 Apr 1.8 1.5 90 0.27 ±2, 5, 10, 20, 30, 40, 50, 60, 70, 80, 90 1928 + 738. 1980 Sep 1.3 1.0 140 1.46 ±1, 2, 3, 4, 6, 8, 10, 20, 30, 40, 50, 60, 70, 80, 90 1954 + 513. 1979 Jul 2.9 2.0 -19 0.71 ±2, 6, 10, 20, 30, 40, 50, 60, 70, 80, 90 2021 + 614. 1979 Dec 2.0 2.0 0 0.90 ±2, 4, 6, 8, 10, 20, 30, 40, 50, 60, 70, 80, 90 2200 + 420. 1978 Dec 2.9 2.4 11 1.20 ±1, ±2, ±3, 4, 5, 10, 20, 30, 40, 50, 60, 70, 80, 90 2351 + 456. 1980 Jul 3.8 0.9 -15 0.27 ±5, 15, 25, 35, 45, 55, 65, 75, 85, 95	1807 + 698						
1828 + 487 1978 Dec 2.9 2.1 10 1.01 ±2.5, 5, 7.5, 10, 20, 30, 40, 50, 60, 70, 80, 90 1845 + 797 1982 Apr 1.8 1.5 90 0.27 ±2, 5, 10, 20, 30, 40, 50, 60, 70, 80, 90 1928 + 738 1980 Sep 1.3 1.0 140 1.46 ±1, 2, 3, 4, 6, 8, 10, 20, 30, 40, 50, 60, 70, 80, 90 1954 + 513 1979 Jul 2.9 2.0 -19 0.71 ±2, 6, 10, 20, 30, 40, 50, 60, 70, 80, 90 2021 + 614 1979 Dec 2.0 2.0 0 0.90 ±2, 4, 6, 8, 10, 20, 30, 40, 50, 60, 70, 80, 90 2200 + 420 1978 Dec 2.9 2.4 11 1.20 ±1, ±2, ±3, 4, 5, 10, 20, 30, 40, 50, 60, 70, 80, 90 2351 + 456 1980 Jul 3.8 0.9 -15 0.27 ±5, 15, 25, 35, 45, 55, 65, 75, 85, 95							
1845+797 1982 Apr 1.8 1.5 90 0.27 ±2, 5, 10, 20, 30, 40, 50, 60, 70, 80, 90 1928+738 1980 Sep 1.3 1.0 140 1.46 ±1, 2, 3, 4, 6, 8, 10, 20, 30, 40, 50, 60, 70, 80, 90 1954+513 1979 Jul 2.9 2.0 -19 0.71 ±2, 6, 10, 20, 30, 40, 50, 60, 70, 80, 90 2021+614 1979 Dec 2.0 2.0 0 0.90 ±2, 4, 6, 8, 10, 20, 30, 40, 50, 60, 70, 80, 90 2200+420 1978 Dec 2.9 2.4 11 1.20 ±1, ±2, ±3, 4, 5, 10, 20, 30, 40, 50, 60, 70, 80, 90 2351+456 1980 Jul 3.8 0.9 -15 0.27 ±5, 15, 25, 35, 45, 55, 65, 75, 85, 95	1828 + 487						
1928 + 738 1980 Sep 1.3 1.0 140 1.46 ±1, 2, 3, 4, 6, 8, 10, 20, 30, 40, 50, 60, 70, 80, 90 1954 + 513 1979 Jul 2.9 2.0 -19 0.71 ±2, 6, 10, 20, 30, 40, 50, 60, 70, 80, 90 2021 + 614 1979 Dec 2.0 2.0 0 0.90 ±2, 4, 6, 8, 10, 20, 30, 40, 50, 60, 70, 80, 90 2200 + 420 1978 Dec 2.9 2.4 11 1.20 ±1, ±2, ±3, 4, 5, 10, 20, 30, 40, 50, 60, 70, 80, 90 2351 + 456 1980 Jul 3.8 0.9 -15 0.27 ±5, 15, 25, 35, 45, 55, 65, 75, 85, 95	1845 + 797	1982 Apr	1 8	1.5			
1954 + 513 1979 Jul 2.9 2.0 -19 0.71 ±2, 6, 10, 20, 30, 40, 50, 60, 70, 80, 90 2021 + 614 1979 Dec 2.0 2.0 0 0.90 ±2, 4, 6, 8, 10, 20, 30, 40, 50, 60, 70, 80, 90 2200 + 420 1978 Dec 2.9 2.4 11 1.20 ±1, ±2, ±3, 4, 5, 10, 20, 30, 40, 50, 60, 70, 80, 90 2351 + 456 1980 Jul 3.8 0.9 -15 0.27 ±5, 15, 25, 35, 45, 55, 65, 75, 85, 95							
2021 + 614 1979 Dec 2.0 2.0 0 0.90 ±2, 4, 6, 8, 10, 20, 30, 40, 50, 60, 70, 80, 90 2200 + 420 1978 Dec 2.9 2.4 11 1.20 ±1, ±2, ±3, 4, 5, 10, 20, 30, 40, 50, 60, 70, 80, 90 2351 + 456 1980 Jul 3.8 0.9 -15 0.27 ±5, 15, 25, 35, 45, 55, 65, 75, 85, 95							
2200+420 1978 Dec 2.9 2.4 11 1.20 ±1, ±2, ±3, 4, 5, 10, 20, 30, 40, 50, 60, 70, 80, 90 2351+456 1980 Jul 3.8 0.9 -15 0.27 ±5, 15, 25, 35, 45, 55, 65, 75, 85, 95							
2351 + 456 1980 Jul 3.8 0.9 -15 0.27 ±5, 15, 25, 35, 45, 55, 65, 75, 85, 95	2200+420						
20, 10, 20, 10, 20, 10, 20, 10, 20, 10, 20, 10, 20, 10, 20, 10, 20, 10, 20, 10, 20, 10, 20, 10, 20, 20, 20, 20, 20, 20, 20, 20, 20, 2	2351 + 456	1980 Iul	3.8				
/31/+491 19/9 LPC 14 111 _36 1157 _17 A S 111 711 30 A0 50 40 70 00 00	2352+495	1979 Dec	1.4	1.0	-36	0.52	±3, 13, 23, 33, 43, 33, 63, 73, 83, 93 ±2, 4, 6, 8, 10, 20, 30, 40, 50, 60, 70, 80, 90

^a The restoring beam is an elliptical Gaussian with FWHM major axis a mas and minor axis b mas, with major axis in position angle θ .

and the model should only be regarded as a *possible* deconvolution of a complex structure. Such deconvolutions are not unique, and can be misleading.

V. CLASSIFICATION

The new observations presented in this paper enable us to classify powerful extragalactic radio sources on the basis of the morphology of the compact radio emission regions close to the

central engine. The objects exhibit a variety of radio morphologies and spectrum shapes. This variety may arise from fundamental differences in the central engine or the host galaxy, or it may be due to environmental effects. A detailed study of the differences may be able to show whether the objects are drawn from a single parent population with a continuum of properties, or whether there are more fundamental differences, and will give us some insight into the relationship between mor-

Notes to Table 2

a Antennas: Only antennas that made successful observations are listed. The source was not detected at stations listed in parentheses. B: 100 m antenna at Effelsberg, near Bonn, Federal Republic of Germany (Max-Planck-Institut für Radioastronomie). F: 26 m antenna at Fort Davis, Texas (George R. Agassiz Station of the Harvard College Observatory). G: 43 m antenna at Green Bank, West Virginia (National Radio Astronomy Observatory). H: 26 m antenna near Cassel, California (Hat Creek Observatory, University of California). K: 37 m antenna near Westford, Massachusetts (Haystack Observatory, Northeast Radio Observatory Corporation). O: 40 m antenna near Big Pine, California (Owens Valley Radio Observatory, California Institute of Technology).

b Polarization: Lin 90—linear, *E*-vector in P.A. 90°. LCP—left circular (IEEE convention).

^c The 1979 April observations were made by R. C. Walker and M. H. Cohen as part of another program.

^d In 1979 November-December K observed right circular polarization.

e In 1980 September antenna G was scheduled but failed.

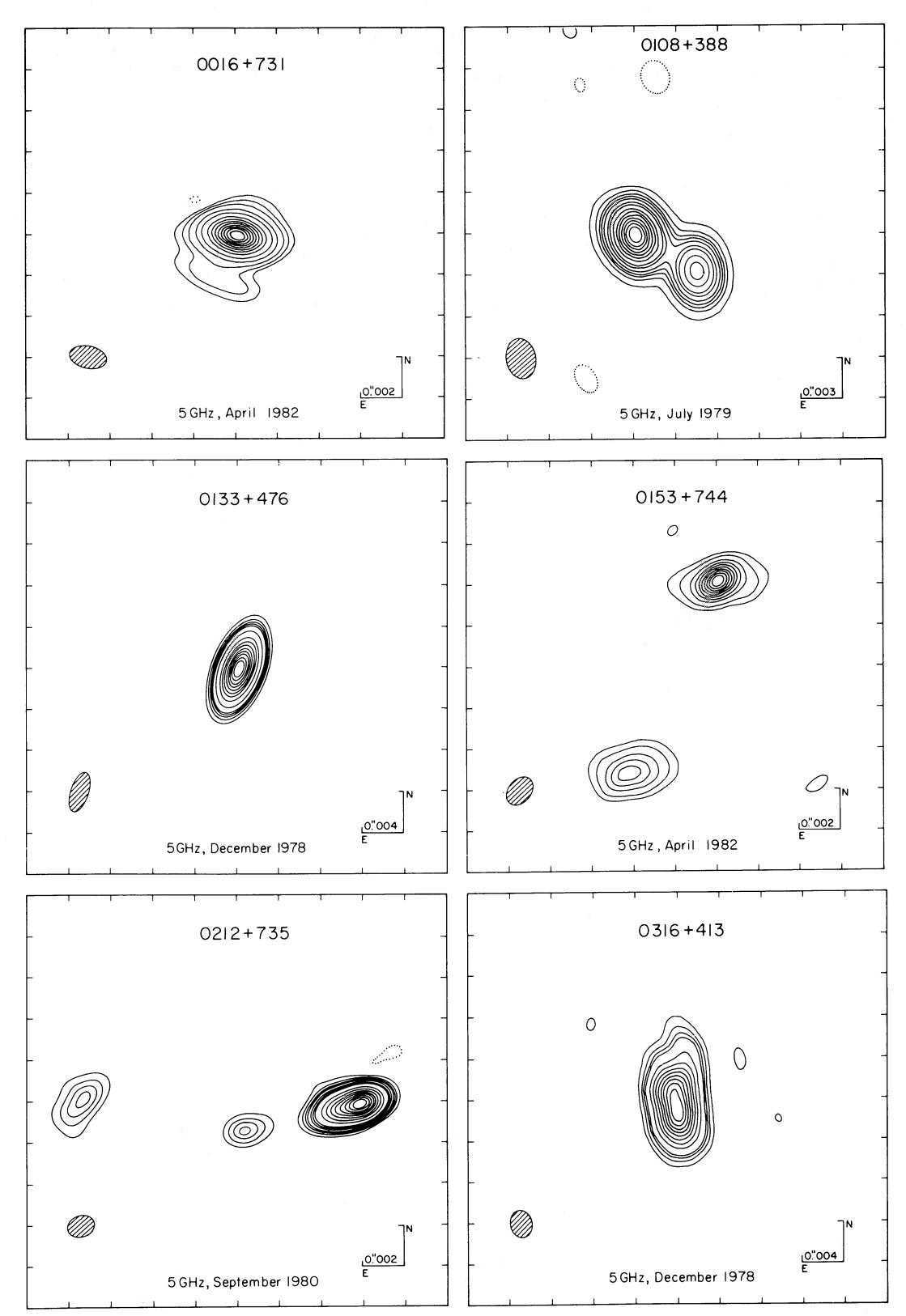
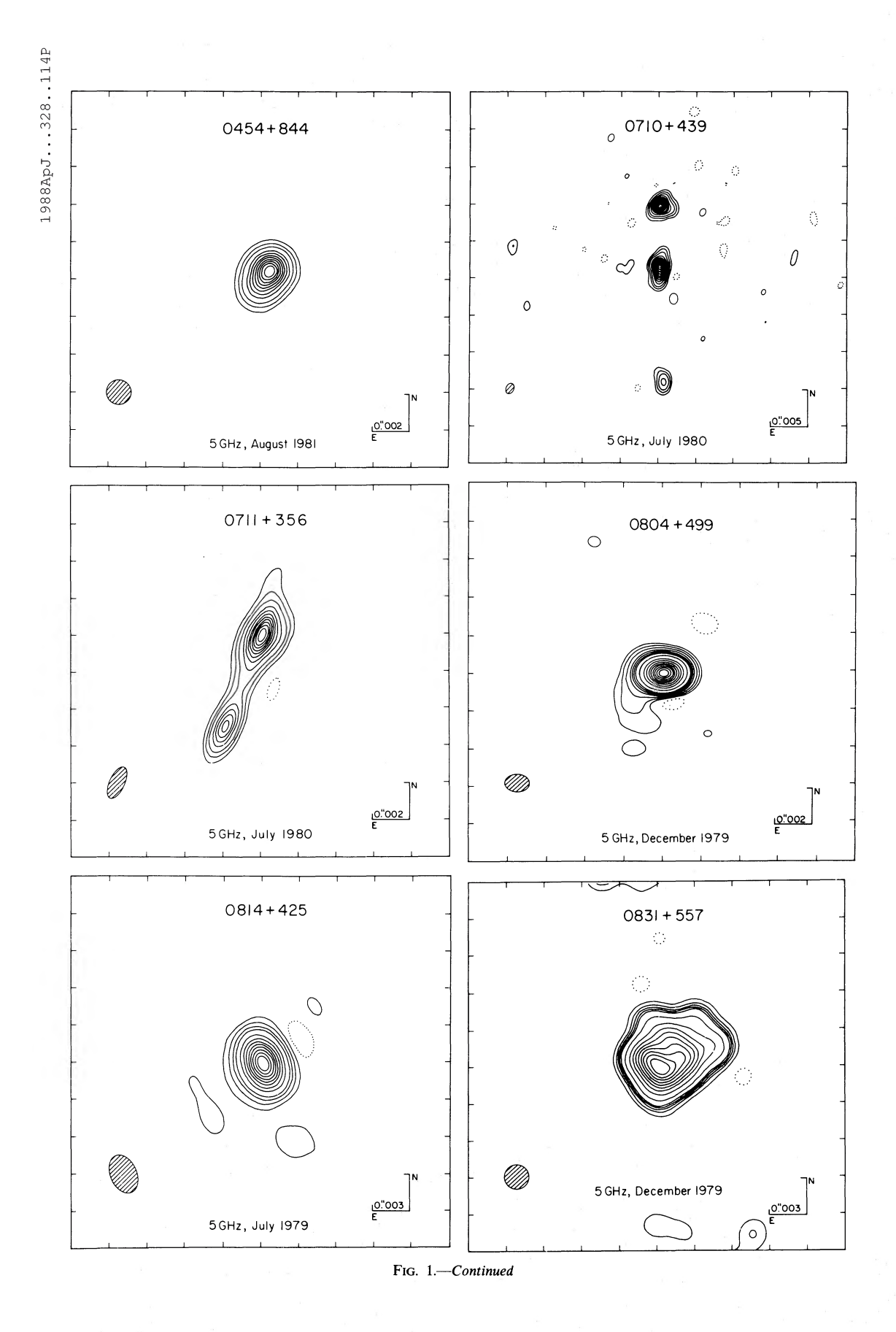
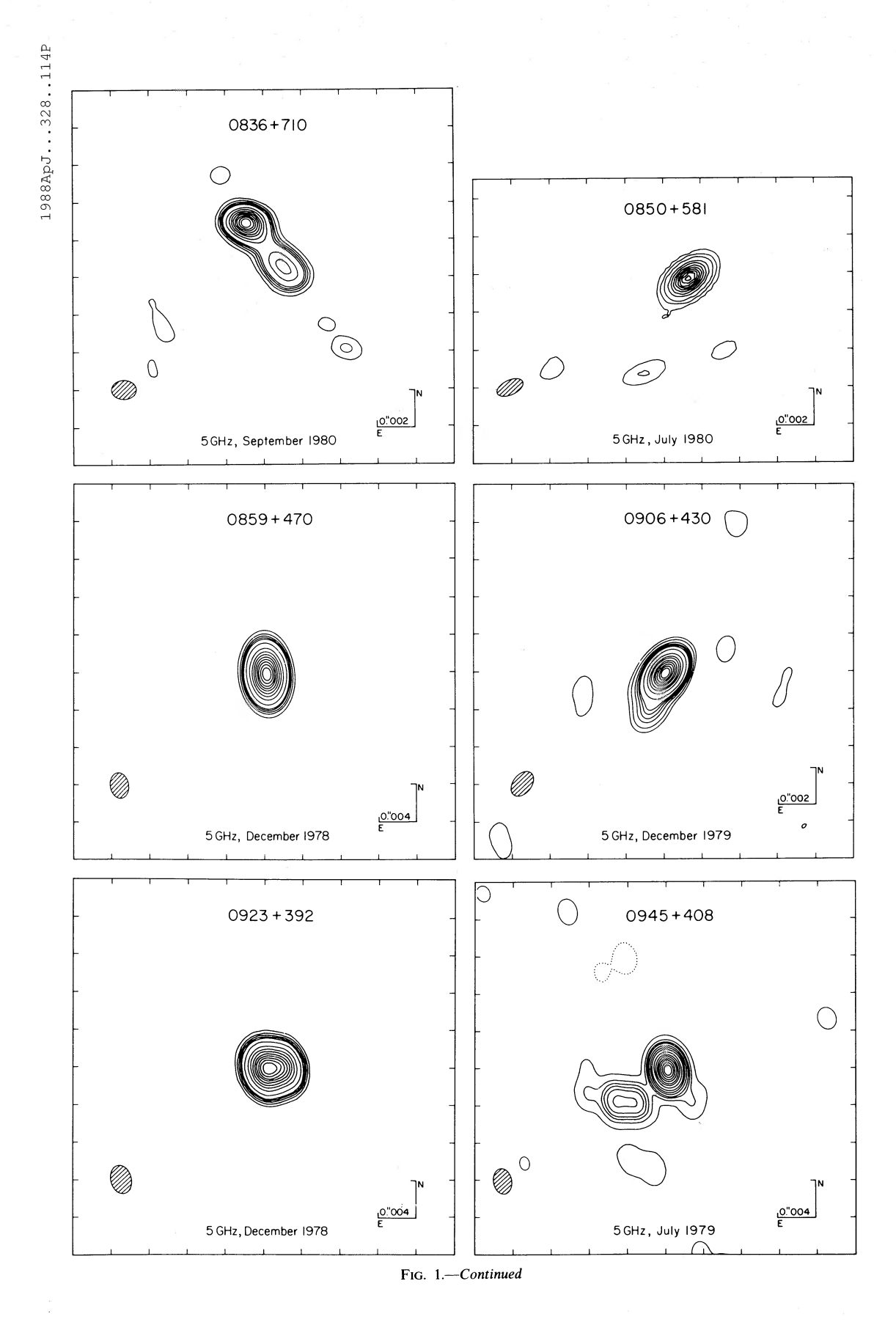


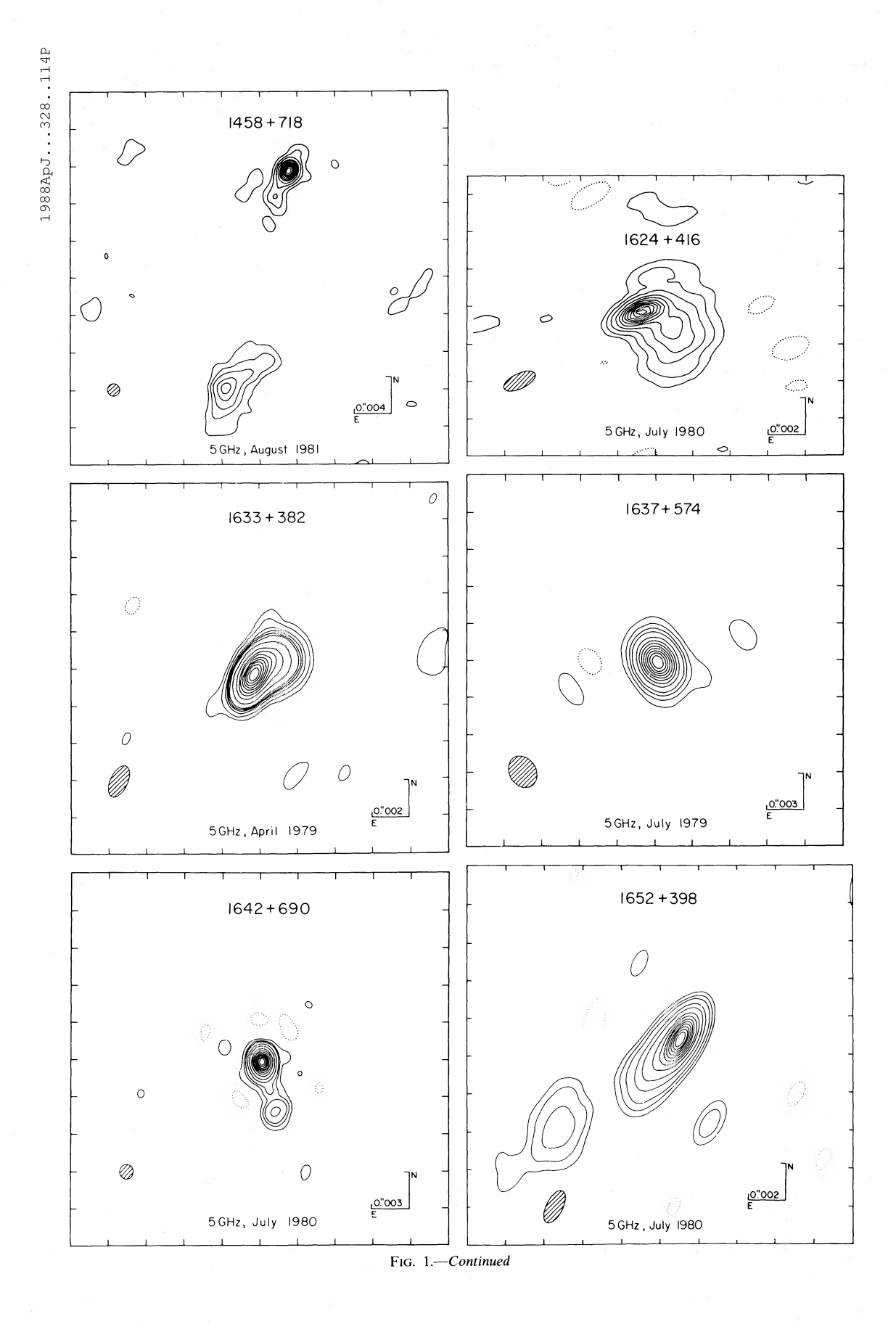
Fig. 1.—First-epoch VLBI maps of 37 sources. The scale of each map is indicated in the lower right-hand corner, and the FWHM contour of the elliptical Gaussian restoring beam is shown as a hatched ellipse in the lower left-hand corner. The peak flux density, contour levels, and parameters of the restoring beam used for each map are listed in Table 3.

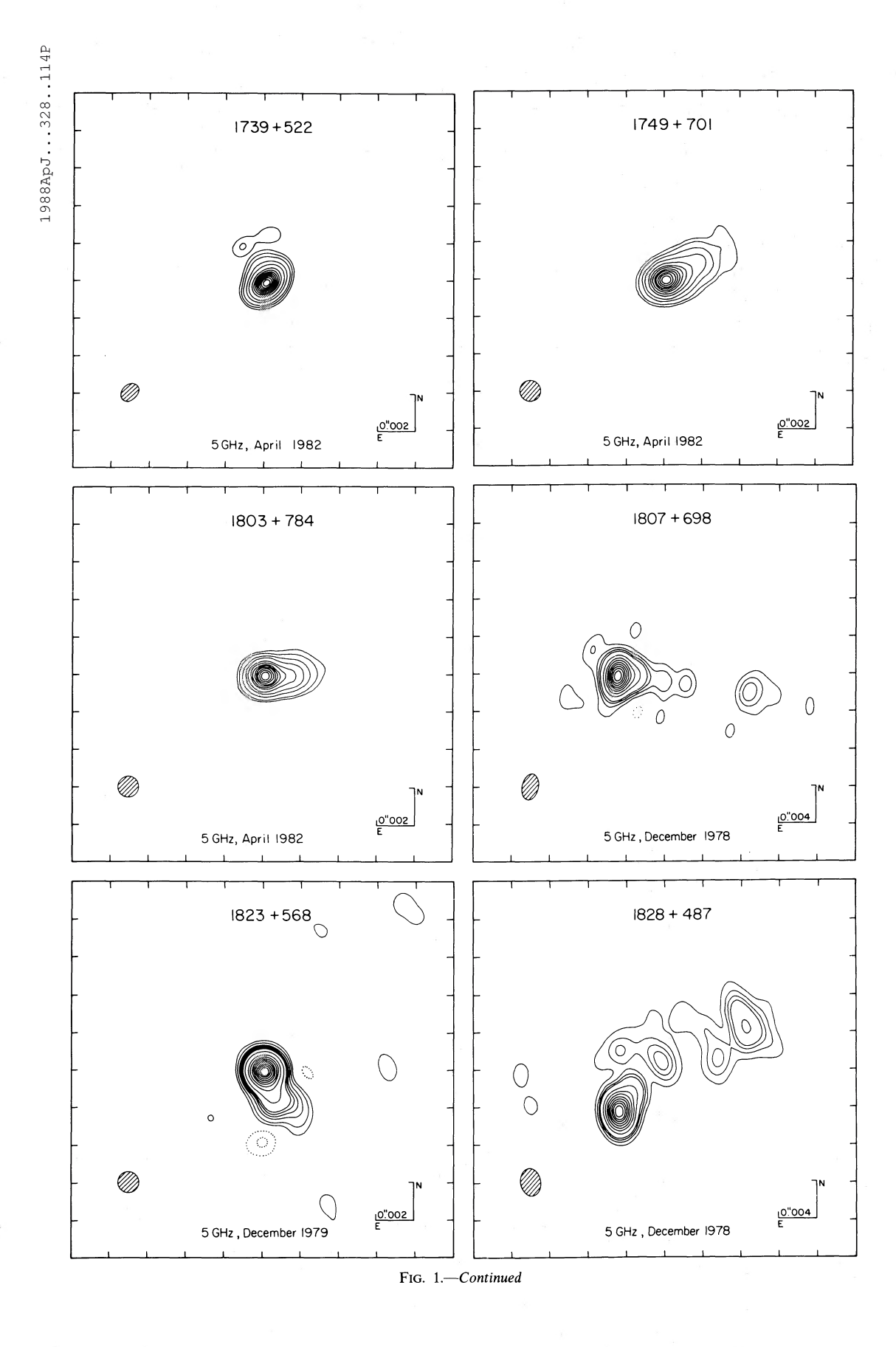


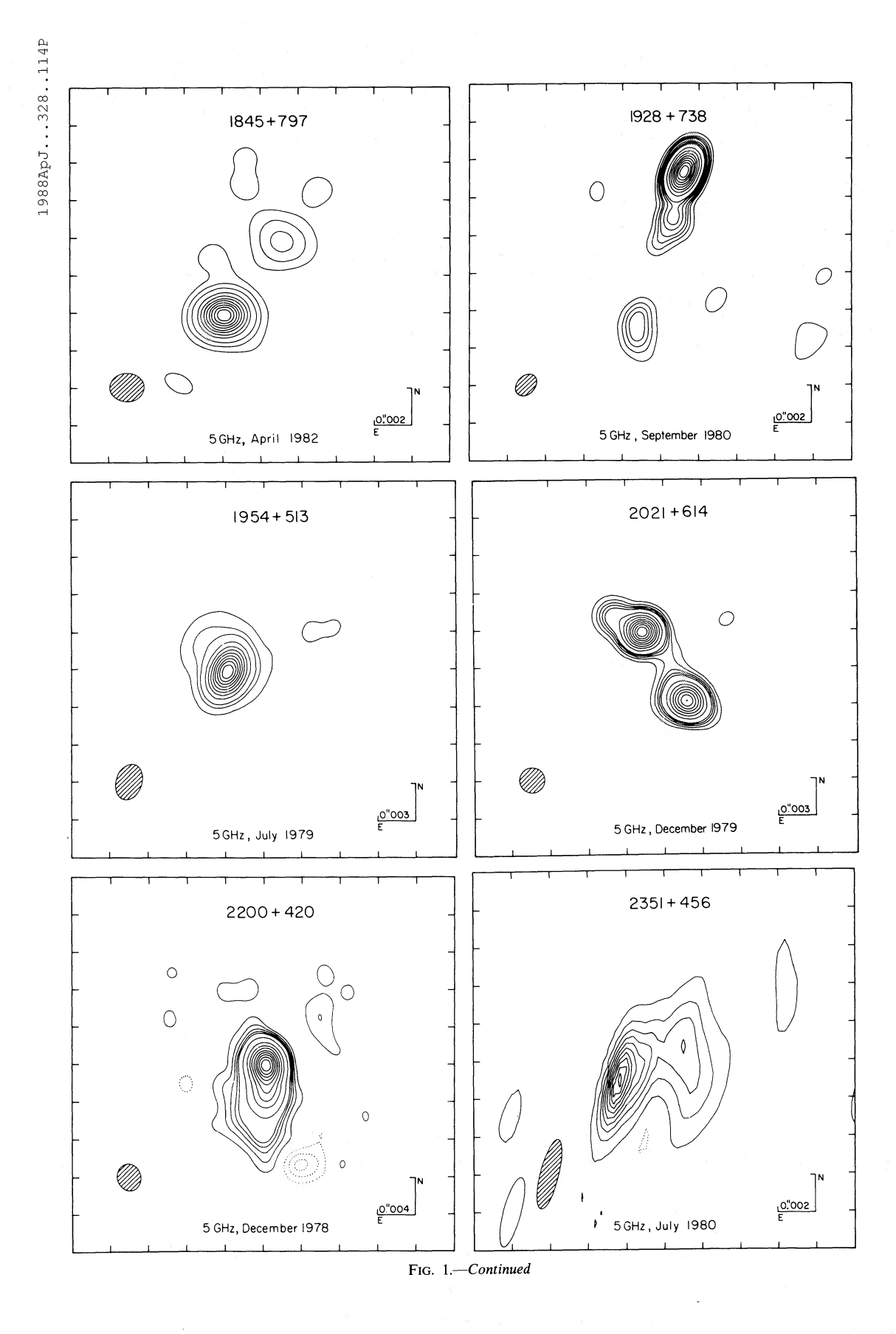
122

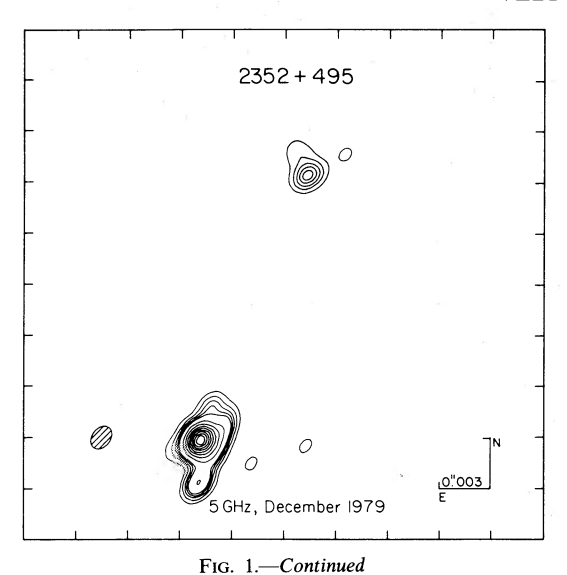


123









phology and the underlying physical processes that may be occurring in the objects.

We have therefore attempted to separate the sources into a number of groups with similar characteristics, based on the VLBI maps of the sources, their large-scale structure, and their radio spectra (Kühr et al. 1981b). Our assignment of these sources to classes is indicated in Table 1 and summarized in Table 5. The classification is based primarily on the morphology of the dominant radio component; we then apply a secondary criterion based on radio spectrum, and, finally, a tertiary criterion based on the size of the dominant radio emission region.

The most obvious distinguishing feature is the presence, or absence, of a strong compact component. It seems likely that the feature with the highest surface brightness is most closely associated with the central engine, and we therefore refer to this as the "core" component. We have used the results of model fitting (see Table 4) to determine the strength of the core, and hence the fraction F_c of the total flux density in the core. In a few objects there are weak unresolved components for which we can derive only lower limits to the surface brightness, but in most of these cases there is also a very high surface brightness feature which dominates the nuclear radio emission and which we identify with the core. Two significant results are that all the cores are situated at one end of the nuclear structure, and they are all resolved, i.e., there is not a single case of a strong compact component which is completely unresolved.

We consider first the sources with $F_c > 0.5$. All these sources have, by definition, a large fraction of their flux density in an unresolved core. We divide them into three classes:

- 1a. Very compact objects $(F_c > 0.9)$;
- 1b. Compact objects $(0.8 < F_c \le 0.9)$;
- 1c. Asymmetric I objects $(0.5 < F_c \le 0.8)$.

All of the objects in these three classes (except perhaps 0859 + 470) are asymmetric, and, as pointed out above, none is completely unresolved. It is possible that they all have a similar asymmetric, "core-jet" structure, and differ only in the relative prominence of the core. All the sources with $F_c > 0.5$ have flat high-frequency spectra ($\alpha > -0.5$ in the range 1-10 GHz, $S \propto v^{\alpha}$), and further subdivision by spectrum is not productive.

Among the objects with $F_c \leq 0.5$, the extended radio emis-

sion is more prominent, and a wider variety of morphologies and spectra are found. We first identify

1d. Asymmetric II objects: these are well-resolved, asymmetric objects with a bright compact component at one end of an extended jetlike feature, and a flat high-frequency spectrum.

A different morphology is exhibited by a class of "compact double" objects, which have two or more well-separated components of comparable brightness. For reasons which will be made clear in § VI, we divide these into two subclasses:

- 2a. Compact S double objects, with a compact double morphology and a steep high-frequency spectrum; these exhibit maxima in their spectra around 1 GHz.
- 2b. Compact F double objects, with a compact double morphology and a flat high-frequency spectrum.

Most of the remaining sources have steep high-frequency spectra. We next select the remaining flat-spectrum sources:

 Irregular flat-spectrum objects: sources with complex milliarcsecond morphology and flat high-frequency spectra.

Finally we divide the remaining steep-spectrum sources according to the extent of the extended emission:

- 4. Steep-spectrum compact objects, in which most of the emission arises in a region with a projected size smaller than 15 kpc.
- 5a. Lobe-dominated objects of Fanaroff-Riley class I;
- 5b. Lobe-dominated objects of Fanaroff-Riley class II.

This completes the classification. It is notable that some possible morphologies do not occur. For example, there are no sources with a flat-spectrum core and two oppositely directed nuclear jets.

VI. TRENDS AND CORRELATIONS

In order to test the physical significance of the morphological classification that we have proposed, we have examined correlations of other observable properties of the sources with morphological class. In this section we discuss the polarization, variability, largest angular size, alignment, and optical identification of the objects in the various classes.

a) Polarization

Measurements of the integrated polarization at 5 GHz of many of the objects in our sample have been made by Perley (1982) and by Rudnick and Jones (1982, 1983). Many of the objects show variations in both polarization strength and position angle, and detailed comparisons with VLBI observations made at a different epoch could be misleading. However, there is a clear difference in the mean level of polarization of objects in different classes (Table 5). Two interesting points should be noted:

- 1. In the very compact, compact, and asymmetric sources the mean level of polarization increases as we progress from class 1a to class 1d, in the direction of increasing prominence of the jet. This suggests that the jets are responsible for most of the observed polarization. This result for a large sample of objects is consistent with the few VLBI polarization images that have been made so far, in which it is found that the jets are polarized and the cores have low levels of polarization (Roberts and Wardle 1987).
- 2. The compact double sources of both classes 2a and 2b have levels of polarization which are, on average, about an order of magnitude below those of the asymmetric objects. This suggests that the basic structures of the compact double

TABLE 4
Gaussian Models

Source	(Jy)	r (mas)	θ (degrees)	a (mas)	b/a	ϕ (degrees)	A.F. (amplitude)	A.F. (closure phase
0016 + 731	1.582 0.091	0.00 1.66	0.0 155.7	0.55 1.84	0.70 0.23	99.6 100.2	2.01	1.16
108 + 388	0.558	0.00	0.0	1.02	0.69	82.1	1.21	1.20
133 + 476	1.156	5.06	59.1	1.41	0.36	65.6	0.07	
133+4/0	1.596 0.199	0.00 3.67	0.0 316.9	1.41 3.90	0.64 0.59	147.6 13.7	0.87	1.17
153 + 744	0.374	4.66	-25.0	0.00	•		5.55	2.12
	0.270 0.620	4.95 5.49	-26.1 157.2	2.65	0.00	93.5 96.3		
212 + 735	1.358	0.00	0.0	2.23 0.79	0.43	118.9	1.75	1.67
	0.529	1.25	103.5	0.74	0.63	137.0		
	0.117 0.062	5.74 14.22	102.9 106.9	1.21 1.72	0.68 0.61	103.7 25.6		
454 + 844	0.523	0.00	0.0	1.16	0.40	-25.3	1.79	0.90
5 10 - 100	0.507	0.83	-36.4	0.15	1.00			4.
710+439	0.625 0.713	8.45 0.00	$-0.1 \\ 0.0$	1.25 2.36	0.59 0.30	90.0 0.0	3.83	4.48
	0.167	15.42	182.2	1.14	0.73	0.0		
711 + 356	0.268	0.00	0.0	0.11	1.00	•••	1.53	1.45
	0.776 0.150	5.35 2.40	-21.7 -25.1	1.21 1.86	0.62 0.26	-23.4 -24.9		
	0.150	5.67	-23.1 -34.6	0.00		- 24.9		
804 + 499	1.344	0.00	0.0	0.23	1.00	!	1.53	1.16
	0.075 0.075	2.78 1.00	140.4 85.9	3.96 1.32	0.32 0.20	0.0		
814 + 425	1.599	0.00	0.0	0.55	0.20	98.4	2.94	1.17
	0.100	1.97	148.7	0.00				
836 + 710	1.045	0.00	0.0	0.75	0.20	35.3	1.63	1.77
	0.554 0.425	1.84 3.35	214.2 220.2	3.00 1.25	0.00 0.57	36.6 42.5		
	0.384	8.40	217.3	3.03	0.47	26.4		
850 + 581	0.936	0.00	0.0	0.87	0.31	162.5	1.14	1.50
859 + 470	0.087 1.151	5.30 0.00	156.1 0.0	0.96 2.14	0.63 0.43	63.7 0.6	1.05	1.10
906 + 430	0.875	0.00	0.0	0.11	0.43	30.8	0.87	1.26
	0.091	1.88	154.5	1.48	0.29	14.6		
923 + 392	4.710	0.00	0.0	1.15	0.96	85.9 14.9	0.82	1.31
945 + 408	2.331 0.746	1.89 0.00	276.9 0.0	0.80 0.50	0.00	- 14.9 97.9	1.61	1.70
	0.363	5.77	127.1	4.40	0.18	83.7		
624 + 416	0.429	0.00	0.0	0.70	0.22	95.0	1.87	1.23
633 + 382	0.688 0.425	2.02 0.00	238.9 0.0	2.84 1.17	0.70 0.24	4.5 138.8	0.58	1.20
033 302	0.857	0.34	115.1	0.00			0.50	1.20
60G · 5G4	0.428	1.08	-63.8	1.16	0.59	-106.3		
637 + 574	1.830 1.625	0.00	0.0 0.0	1.02 0.73	0.00	7.1 1.9	2.65 3.77	1.11 2.43
042 + 030	0.158	4.23	194.9	1.40	0.38	121.9	3.77	2.43
	0.087	0.97	206.1	0.75	0.00	87.8		
652 + 398	0.449 0.320	0.00	0.0	0.35	0.42	135.1	1.71	1.41
	0.320	0.98 7.93	133.3 127.6	2.47 6.51	0.33 0.32	134.6 124.8		
739 + 522	0.891	0.00	0.0	0.40	0.84	-22.9	1.26	0.98
749 + 701	0.074	1.74	3.2	2.14	0.88	-17.9	1.41	1.16
/49 + /01	0.836 0.432	0.00 1.13	0.0 - 64.3	0.61 2.01	0.00 0.38	-75.4 -56.1	1.41	1.16
803 + 784	2.157	0.00	0.0	0.16	0.00	-93.8	2.67	1.37
007 . 600	0.696	1.24	-92.2	0.87	0.38	-80.2	0.06	
807 + 698	0.952 0.200	0.00 14.13	0.0 - 96.8	0.93 4.10	0.72 0.54	-115.0 -82.0	0.96	1.14
	0.287	1.79	-90.7	2.19	0.00	-94.0		
000 500	0.165	5.72	-102.0	4.61	0.00	-100.0		
823 + 568	1.132	0.00	0.0	0.35	0.00	16.4	1.28	1.24
845 + 797	0.146 0.309	1.35 0.00	197.4 0.0	0.82 0.80	0.00 0.39	23.0 -49.7	1.15	1.05
	0.073	4.86	-37.5	1.71	0.47	-43.4		1.55
928 + 738	2.114	0.00	0.0	1.16	0.18	164.0	2.23	1.42
	0.168 0.202	1.98 3.57	166.0 163.0	1.30 2.03	0.40 0.38	- 24.3 145.6		
	0.202	8.25	163.0	1.90	0.55	- 1.6		
	0.111	16.23	173.0	2.14	0.85	13.5		

TABLE 4—Continued

Source	S (Jy)	r (mas)	θ (degrees)	a (mas)	b/a	θ (degrees)	A.F. (amplitude)	A.F. (closure phase)
954 + 513	0.854	0.00	0.0	1.22	0.76	-50.1	1.28	1.76
,,,,,,,,,,,,,,,,,,,,,,,,,,,,,,,,,,,,,,,	0.217	3.44	7.8	7.23	0.20	-60.9		
2021 + 614	1.012	0.00	0.0	0.77	0.61	57.0	1.33	1.78
2021 0211111111111	0.997	6.57	212.4	1.45	0.70	48.4		
	0.162	2.66	63.8	1.00	0.58	61.0		
200 + 420	1.186	0.00	180.0	0.53	1.00	•••	1.06	1.47
200 1201111111	0.648	2.99	182.7	1.63	1.00			
	0.154	6.70	173.8	2.97	1.00			
2351 + 456	0.323	0.00	0.0	0.77	0.80	-56.0	1.52	1.88
	0.166	1.46	-72.9	1.04	0.71	-48.1		
	0.302	3.88	-62.2	2.35	0.62	-10.7		
2352 + 495	0.730	0.00	0.0	0.86	0.90	54.9	2.44	2.93
,,,,,,,,,,,,,,,,,,,,,,,,,,,,,,,,,,,,,,,	0.212	2.13	177.8	1.05	0.00	0.2		
	0.146	16.77	-21.7	1.18	0.83	105.6		

Note.—Parameters of each elliptical Gaussian component of the model brightness distribution: S, flux density; r, θ , polar coordinates of the center of the component relative to an arbitrary origin, with polar angle measured from north through east; a, b major and minor axes of the FWHM contour; ϕ , position angle of the major axis, measured from north through east. The agreement factors (reduced χ^2) between the model and the data are denoted by A.F. (amplitude) and A.F. (closure phase). The following sources were too complex for modeling: 0316+413,0831+557,1458+718,1828+487.

sources are different from those of the core-jet sources; e.g., the observed features are probably not parts of invisible underlying jets.

In an inhomogeneous sample of 26 radio sources, Rusk and Seaquist (1985) found a strong trend for the *E*-vector of the radio polarization to lie normal to the VLBI structural axis. Rusk (1987) has suggested that there is a difference between BL Lac objects, in which the polarization tends to lie parallel to the structural axis, and quasars and radio galaxies, in which the polarization tends to lie normal to the axis. In our sample the distribution is bimodal, with the polarization position

angles tending to lie either perpendicular or parallel to the structural axis. However, only a small number of sources have data of sufficient quality for this investigation, and more observations of the polarization of the cores of the objects and their Faraday rotation measures are needed before a definitive statement can be made.

b) Variability

Seielstad, Pearson, and Readhead (1983) measured the 10.7 GHz flux density variability over a period of 4 years of all the sources in our sample south of declination 70°. Their

TABLE 5
CLASSIFICATION OF THE 65 SOURCES IN THE COMPLETE SAMPLE

Class	Description	Core Fraction F_c	Number	Members	Mean Polarization (5 GHz) ^a	Fraction with $V > 0.4^{a}$
1a	Very compact	$0.9 \le F_c < 1.0$	4	0016 + 731, 0804 + 499, 1637 + 574, 1739 + 522	1.6 ± 0.5 (4)	1.00 (3)
1 <i>b</i>	Compact	$0.8 \le F_c < 0.9$	4	0133 + 476, 0814 + 425, 0850 + 581, $1642 + 690$	1.4 ± 0.9 (4)	1.00 (4)
1 <i>c</i>	Asymmetric I	$0.5 \le F_c < 0.8$	9	0212+735, 0454+844, 0859+470, 1749+701, 1803+784, 1823+568, 1928+738, 1954+513, 2200+420	2.9 ± 1.8 (9)	0.80 (5)
1 <i>d</i>	Asymmetric II	$F_c < 0.5$	8	0836+710, 0945+408, 1624+416, 1633+382, 1641+399, 1652+398, 1807+698, 2351+456	3.3 ± 2.6 (8)	0.43 (7)
2a	Compact S double	$F_{c} < 0.5$	3	0108 + 388, 0710 + 439, 2352 + 495	0.3 ± 0.1 (3)	0.00(3)
2 <i>b</i>	Compact F double	$F_c^c < 0.5$	4	0153 + 744, 0711 + 356, 0923 + 392, 2021 + 614	0.5 ± 0.4 (4)	0.33 (3)
3	Irregular flat-spectrum	$F_{c} < 0.5$	2	0316 + 413,0831 + 557	0.1 ± 0.1 (2)	•••
4	Steep-spectrum compact	$F_c < 0.5$	7	0404 + 768, 0538 + 498, 0906 + 430, 1458 + 718, 1634 + 628, 1828 + 487, 2342 + 821	2.4 ± 2.2 (4)	0.00 (4)
5 <i>a</i>	Lobe-dominated, F-R I	$F_{c} < 0.5$	3	0220 + 427, 0314 + 416, 2229 + 391	• • • •	
5b	Lobe-dominated, F-R II	$F_{c}^{c} < 0.5$	16	0040 + 517, 0210 + 860, 0605 + 480,	• • •	
30	2000 dominates, 1 10 11	2		0723+679, 0809+483, 0917+458, 1003+351, 1157+732, 1254+476, 1409+524, 1609+660, 1842+455,		
				1845 + 797, 1939 + 605, 2153 + 377, 2243 + 394		
	Not classified (M82)		1	0951 + 699		
	Not yet observed	*	4	0954 + 556, 0954 + 658, 1031 + 567, 1358 + 624	··· * *	- 1

^a Number of sources for which data are available given in parentheses.

results show that there is a clear difference in the variability of the sources in the different classes. Rather than estimate the "mean variability" in each class, which is rather sensitive to the behavior of a few highly variable sources, we have determined the fraction of objects in each class for which the fractional variability estimated by Seielstad et al., $V = \Delta S/\langle S \rangle$, is greater than 0.4 (Table 5). The great majority of compact and asymmetric sources in classes 1a-1c are variable at this level, but a significantly smaller fraction of the sources in class 1d ("asymmetric II") exceed this level. Very few of the compact double sources (classes 2a and 2b) or steep-spectrum compact sources (class 4) exceed this level of variability.

Only the most compact emission regions are expected to be variable on a time scale of 4 yr. Thus the lower level of variability in objects of class 1d can be attributed to the greater prominence of the resolved jet components in these objects. The projected sizes of these features are greater than a few parsecs, and therefore they have a number of different emission regions separated by distances of this order. Thus we would expect variations in brightness of the different components to occur at different times even if they are causally connected. The same explanation applies to the low variability of the steep-spectrum compact objects (class 4) in which the dominant emission regions are also large.

The low variability observed in the compact double sources, which contain two small dominant emission regions, cannot be explained in this way. It appears that the low variability must be an intrinsic feature of these objects, again suggesting that they are intrinsically different from the core-jet sources.

c) Largest Angular Size

We have collected information on the largest angular size of the objects in our sample from the literature. The references are given in the Appendix. In recent years, very high dynamic range maps made with the VLA and MERLIN have revealed low-level extended structure in many of the objects, and we can expect that further observations will find more. In every morphological class except for 2a (the steep-spectrum compact doubles), some sources have low-brightness features considerably larger than 1". This is true even of the very compact objects. Among the compact double sources, however, only one, 0923+395 (4C 39.25), has a largest angular size greater than 0".2. This source has some similarities to the asymmetric core-jet sources, e.g., it shows superluminal motion, and it raises doubts as to whether the flat-spectrum compact doubles should not be considered more akin to the asymmetric sources than to the steep-spectrum compact doubles.

d) Alignment of Large-Scale and Small-Scale Structures

It is generally believed that the small-scale jets observed in VLBI images are the sources of, and are continuous with, the large-scale jets that supply the outer lobes. To investigate this hypothesis, we have compared the position angle of the radio structure revealed in the VLBI maps with the position angle of the larger scale structure. The distribution of the differences between these two angles reflects the distribution of the deviations of the jets from straight lines, and, in the beaming picture, larger deviations should be observed in the sources with stronger cores, owing to projection effects (e.g., Moore et al. 1981; Readhead et al. 1983; Readhead, Pearson, and Barthel 1987). The observed distribution is sensitive to both the magnitude of the intrinsic deviations and the Lorentz factor of the jets, but it is not possible to disentangle these two

 $\begin{tabular}{ll} TABLE & 6 \\ A LIGNMENT OF LARGE-SCALE AND SMALL-SCALE STRUCTURE \\ \end{tabular}$

Source	Large-Scale P.A.	Small-Scale P.A.	Difference Δ(P.A.)
$0723 + 679 \dots$	260°	272°	12°
$0836 + 710 \dots$	204	214	10
$0850 + 581 \dots$	139	156	17
$0906 + 430 \dots$	241	155	86
$0923 + 392 \dots$	259	277	18
$0945 + 408 \dots$	32	127	95
$1003 + 351 \dots$	304	292	12
$1458 + 718 \dots$	73	164	91
$1624 + 416 \dots$	351	239	112
$1641 + 399 \dots$	328	230	98
$1642 + 690 \dots$	168	195	27
$1749 + 701 \dots$	209	296	87
$1803 + 784 \dots$	195	268	73
$1807 + 698 \dots$	241	263	22
$1823 + 568 \dots$	98	197	99
$1828 + 480 \dots$	316	328	12
$1845 + 797 \dots$	323	322	1
1928 + 738	189	166	23

contributions on the basis of the misalignments alone (Rusk and Rusk 1986).

In Table 6 we list the 18 objects in the sample for which both a small-scale and a large-scale position angle are available. For the small scale we have taken the position angle of the feature closest to the VLBI core (the brightest, most compact component in the map), while for the large scale we have taken the position angle relative to the core of either a portion of the large-scale jet or a compact hot spot, choosing the angle which maximizes the position-angle difference $\Delta(P.A.)$ between the inner and the outer structure. The resulting distribution of position-angle differences (Fig. 2) is remarkable and quite unexpected. There are two distinct peaks in the distribution, one at zero as expected if intrinsic misalignments are small, and a second centered at 90°. The peak at 90° is difficult to explain, but if it is a real feature of the parent population of radio sources, it could provide an important constraint on models of the jet, the central engine, and the host galaxy.

In a similar study of a larger, inhomogeneous sample (including many of the sources in Table 6), Rusk and Rusk (1986) found a smooth distribution of $\Delta(P.A.)$ peaked at zero. This suggests that the bimodal distribution found in our sample could be due to statistical fluctuation, or it could be a result of the different selection criteria. A chi-square test of the null hypothesis that both samples are taken from the same parent population shows that the differences between the two samples are not statistically significant. The bimodality of our distribution is sufficiently striking, however, to encourage us to investigate the implications of a real preference for $\Delta(P.A.)$ values close to 90°.

It is straightforward to calculate the expected distribution of $\Delta(P.A.)$ for a given intrinsic bend between the inner and the outer jets, both when relativistic beaming is a dominant effect and when it is not. The expected distribution is always peaked around the intrinsic angle of bend in the nonrelativistic case, although the distribution is broadened by projection (examples for intrinsic bends of 15° and 90° are shown in Fig. 2). If relativistic beaming is important, the peak is broadened, the width increasing with Lorentz factor γ , and an almost uniform distribution is obtained if $1/\gamma$ is smaller than the intrinsic angle of deviation. (If relativistic beaming is important in the large-scale

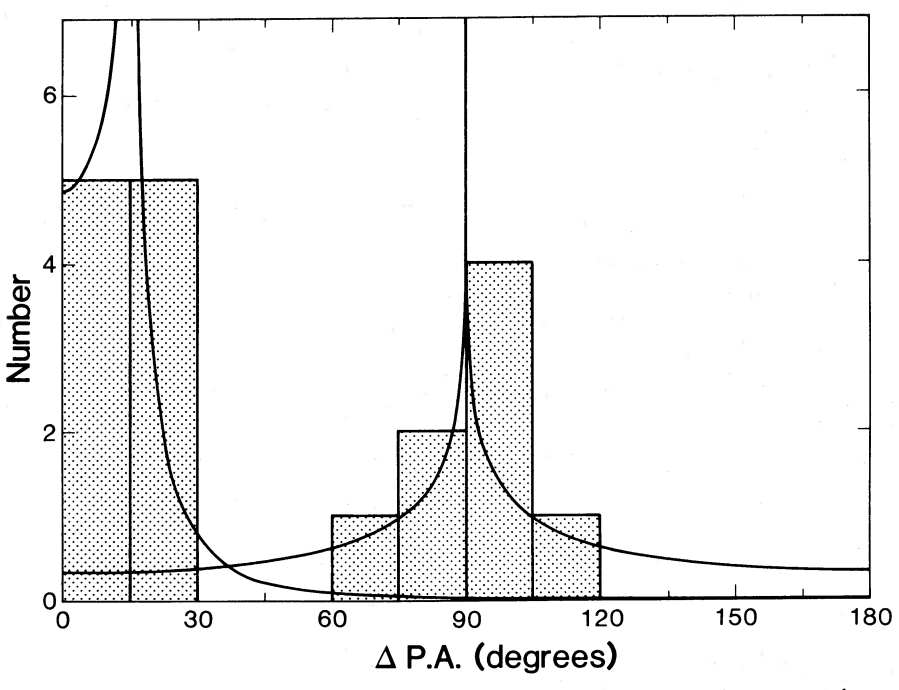


Fig. 2.—Distribution of the absolute value of the difference in position angle $\Delta(P.A.)$ between small-scale (VLBI) structure and extended structure, in the sample of 18 sources for which information is available (Table 6). Two theoretical probability distributions are plotted, assuming that the objects are randomly oriented with respect to the line of sight and that they all have the same intrinsic bend angle (15° and 90° for the two distributions). The probability distributions are normalized to 10 objects (15° curve) and eight objects (90° curve), in accordance with the apparent distribution of objects between the two peaks.

structure, however, observational selection will discriminate against objects in which the emission from large-scale structure is beamed away from the line of sight. Such effects are very model-dependent.) Other effects will also broaden the distribution, including a distribution of intrinsic bend angles and observational errors. We conclude that in order to produce a sharp peak in the distribution around $\Delta(P.A.) \sim 90^{\circ}$, the sources must have an intrinsic bend angle of 90° , with little variance, and relativistic beaming cannot introduce a strong orientation bias in the observed sample.

It is difficult to conceive of mechanisms for bending jets that will result in a preferred intrinsic misalignment of 90° between the small-scale and large-scale structure. For example, models which attribute the bending to precession of the central engine have no preferred misalignment. If the jets are bent by a pressure gradient in the host galaxy, then we can identify the axis of the large-scale structure with that of the galaxy pressure gradient, while the axis of the small-scale structure is that of the central engine (black hole). With this interpretation, our observations would suggest that there is a class of sources in which these two axes are perpendicular.

It is therefore important to test the reality of the bimodal distribution by observing larger, independent samples, and by making high dynamic range maps with resolution 0".1–1" of the objects in our sample for which large-scale structure has not yet been detected.

e) Optical Identification and Spectrum

The published optical data on the objects are very inhomogeneous, and, in particular, there has been no systematic attempt to distinguish between quasars and BL Lac objects. We have nearly completed a program (with C. R. Lawrence and S. C. Unwin) to obtain high-quality spectra of all the objects using the Palomar 200 inch telescope, which we hope

will improve the situation. With such information as is available, some trends are apparent. Approximately 75% of the core-dominated sources for which we have maps are quasars or BL Lac objects. It is therefore notable that all 17 of the sources in classes 1a, 1b, and 1c are quasars or BL Lac objects, and even more remarkable that all three of the steep-spectrum compact double sources are identified with galaxies. Here we also see a distinction between the flat-spectrum and the steep-spectrum compact doubles: only one out of the four flat-spectrum compact doubles is identified with a galaxy.

VII. DISCUSSION

In this section we discuss the different classes of object in more detail.

a) Very Compact and Compact Sources

The very compact and compact sources have, by definition, a single unresolved component (smaller than a milliarcsecond) which emits > 80% of the flux density. All the sources in these two classes are highly variable, changing by 50% or more in 4 yr or less (at 10.7 GHz). All are fairly strongly polarized (>1%), and all are quasars.

The "very compact" sources can be regarded as "naked cores," that is, flat-spectrum core sources without an associated jet; and it is possible that we shall find a jet by making images of higher dynamic range, or by making images when these highly variable sources are in a low state. In some cases the images show some low-brightness emission at a very low level, <1% of the peak, but this is at the limit of the VLBI imaging process. (These sources are thus good phase calibrators for VLBI arrays.)

The "compact" sources are intermediate between the "very compact" sources and the "asymmetric" sources. Where low-brightness nuclear emission is found, it is one-sided. At least

two "compact" sources are known to be superluminal (0850+581: Barthel et al. 1986; 1642+690: Pearson et al. 1986), and it is likely that others will be found to be superluminal, although in some cases the observations are very difficult owing to the high dynamic range required.

b) Asymmetric Sources

The asymmetric I sources are defined, analogously to the compact sources, by the relative strength of the unresolved core, which is between 50% and 80% of the total flux density. All of these sources have an asymmetric structure with a compact core and a lower brightness extension (or "jet") on one side only. The asymmetric II sources are defined by morphology; the one-sided structure is similar to that of the asymmetric I sources, but the fraction of flux density in the core is <50%. In the few sources for which spectral information is available, the core is found to have a flat (self-absorbed) spectrum and the "jet" a steeper spectrum.

It is possibly misleading to use the word "jet" to describe the asymmetric features in these sources. It is reasonable to use it for the long linear structures seen in objects like Cygnus A and NGC 6251, where there must be a flow of material along the jet to supply the energy requirement of the outer lobes. In the VLBI sources, the word is used to describe almost any feature that is slightly longer than it is wide, with no evidence for any material flow at all. The justification comes from the analogy—and at this stage it is only an analogy—between these sources and the few where there is good evidence for a jet; the evidence is (1) continuity of the parsec-scale VLBI structure with a large-scale jet supplying an outer lobe and (2) apparent bulk relativistic motion outward along the jets in superluminal sources.

Many of these sources have extensive large-scale structure. Although they were at first thought to be small sources of subgalactic dimensions, very high dynamic range observations with the VLA and MERLIN have shown up extensive large-scale features. In some cases the VLBI structure is well aligned with outer arcsecond-scale structure (e.g., 1807+698); in others, the misalignment can be as large as 90° (e.g., 0945+408). Lack of alignment does not imply that there is no connection, however, as 3C 345 illustrates (Browne et al. 1982a). Sometimes, as in 1823+568, the large-scale "jet" seen in the VLA map is highly contorted, but even in these cases the milliarcsecond VLBI jet appears to be connected to the large-scale jet. Note that in all the "asymmetric" sources where there is a large-scale jet, the milliarcsecond jet is either on the same side as the large-scale jet or it connects up with the large-scale jet.

The "prototype" source of this class is 3C 345, the well-known superluminal, which is also in the sample. Another superluminal source in the asymmetric class is 1928+738 (Eckart et al. 1985). It is likely that many more of the asymmetric and compact sources—possibly all of them—will be found to be superluminal when they are studied sufficiently carefully. The similarities between the asymmetric source 1928+738 and the two superluminal sources in the "compact" class emphasize that the distinction between the two classes is probably artificial. In all three cases there is a compact core, and one or more weaker components moving superluminally away from the core. The direction of superluminal expansion is in all cases closely aligned with a kiloparsec-scale jet. What is perhaps most remarkable is that all three sources have a very similar large-scale structure. The VLA images show (1) a

bright, dominant, unresolved core—this is the feature that we are resolving in the VLBI images; (2) a curved continuous jet on one side—in all cases, this is contiguous with the VLBI jet; and (3) a diffuse lobe on the *opposite* side of the core. The overall angular sizes are similar to those of the "classical double" radio galaxies and quasars, which have a similar structure but with a much weaker core. The similarity of the structures suggests that they are related.

c) Compact Double Sources

Unlike previous authors, we have distinguished two different classes of compact double sources: one with steep highfrequency spectra, called compact S doubles or class 2a, and one with flat high-frequency spectra, called compact F doubles or class 2b. The clearest result of the correlations discussed in § VI is that the compact double sources, and particularly the steepspectrum ones, stand apart from the other objects in our sample in almost every respect: (1) they do not look like parts of one- or two-sided jets, whereas all of the other categories do fit this simple model; (2) they have an order of magnitude less polarization; (3) they exhibit a very low level of variability; and (4) they have no detectable structure on the scale of a second of arc. In the compact S doubles, we see no evidence of a compact core, and we conclude that in these objects we are not seeing emission from a core and jet. In the case of the compact F doubles this is not so clear. For example, 0711+439 has a compact flat-spectrum component at one end, and this could therefore be a one-sided jet. We believe that the distinction between these two types of compact double is real.

Compact double sources were first identified as a distinct class by Phillips and Mutel (1982). Phillips and Mutel, with their colleagues, have made an intensive study of four members of the class (Phillips and Mutel 1980, 1981, 1982; Mutel, Phillips, and Skuppin 1981; Phillips and Shaffer 1983; Hodges, Mutel, and Phillips 1984; Mutel, Hodges, and Phillips 1985; Biretta, Schneider, and Gunn 1985; Mutel and Hodges 1986; Hodges and Mutel 1987). In these four sources the radio emission comes from two, roughly equal, well-separated components, 50-150 mas apart; both components have similar spectra, and there is no obvious compact flat-spectrum core. A distinctive feature is that all these sources have "humped" spectra, with a peak at about 1 GHz, a steep falloff to higher frequencies ($\alpha \gtrsim 1$), and little emission at low frequencies. They therefore fall into the class that we call "compact S doubles." At higher resolution some of the components show internal structure; for example, in 2050+364 the two components show "tails" pointing back toward the center. This has led Phillips and Mutel to suggest that these may be "infant" classical double radio sources, in which we are seeing the two heads of two counterprojecting beams, that have not yet escaped from the parent galaxy. In that case, we might expect to see a central component in the middle, marking the central engine; no such components have yet been seen, but that may just be because they are too faint.

In the compact S doubles, the correlation between humped spectrum, low variability, and low polarization that we discussed in § VI was first noticed by Rudnick and Jones (1982). While all our compact S doubles have humped spectra, the converse is not true; sources with such spectra can show a variety of structures. Our observations suggest that both morphology and spectrum must be taken into account in defining this class.

The class of compact F doubles is rather less well defined.

The sources in this class share some, but not all, of the distinguishing features of the compact S doubles. It is not clear whether the class is homogeneous or is an accidental mixture of sources of a variety of types.

d) Irregular Flat-Spectrum Sources

These are flat-spectrum sources with complex resolved structures that can be classified neither as "asymmetric" nor as "double." Only two sources fall into this class, 0315+413 (3C 84) and 0831+557. Both are peculiar (see the notes in the Appendix), but perhaps the only thing they have in common is that they cannot be placed in any of the other classes. At higher frequencies 3C 84 shows many of the characteristics of the asymmetric II class (Readhead et al. 1983).

e) Steep-Spectrum Compact Sources

Seven sources are classified as steep-spectrum compact sources. These sources are characterized by a steep, straight spectrum, usually with a low-frequency turnover near 100 MHz, and sometimes flattening at high frequencies. The spectrum indicates that if such a source has a core, it is much less prominent than in the flat-spectrum sources. This class of sources has been studied by several investigators (e.g., van Breugel, Miley, and Heckman 1984; Fanti et al. 1985). These sources are quite common; for example, Peacock and Wall (1982) studied a sample of 168 sources selected at 2.7 GHz. Contrary to their expectations, they found that a large proportion (44%) of the compact sources (smaller than 2") in their sample had steep high-frequency spectra. (Selection by spectrum alone would also find the compact S doubles; in the current sample, 10 out of 65 [15%] fall into one of the two classes with steep high-frequency spectra.)

The steep-spectrum compact sources show structure on all angular scales from 1 mas to 1". The VLBI structure is complex, showing a compact, flat-spectrum core, and in some cases a central "jet" which may be misaligned by as much as 90° from the large-scale structure. These sources are unlikely to be normal extended double sources seen "end-on," because in many cases no flat-spectrum core is observed and the overall sizes are smaller than the lobe widths of normal double sources (though 3C 380 may be an exception). There is some evidence from inverse-Compton arguments that relativistic bulk motion is occurring in two of these sources (3C 147 and 3C 309.1; Simon 1982; Wilkinson et al. 1986) and superluminal motion has been detected in 3C 216 (Pearson, Readhead, and Barthel 1987).

f) Lobe-dominated Sources

We have classified 19 of the sources in the complete sample as "lobe-dominated." Three of these are low-luminosity sources of Fanaroff-Riley class I, and 16 are high-luminosity "classical" sources of class II. Almost all such sources have a compact core associated with the parent galaxy or quasar. Most of the cores are very weak, however, <100 mJy at 5 GHz, and we detected VLBI fringes from only the three strongest. The results are thus biased toward sources with unusually strong central components. Two of the three sources, 3C 179 and 3C 236, were excluded from our observations because they have been extensively studied by others (see § IV); the third is 3C 390.3, which has also been mapped by Preuss et al. (1980) and Linfield (1981). All three sources show good alignment between the nuclear structure and the outer lobes. One (3C 179) is definitely superluminal (Porcas 1981),

and another (3C 390.3) may be (see the notes in the Appendix). It is of interest that 3C 390.3 shows possible evidence for two-sided ejection: Linfield's 10.7 GHz map shows a "core-jet" structure directed toward the bright, compact southeast lobe, while both our 5 GHz map and that of Preuss *et al.* show another component 5 mas away on the northwest side of the "core."

g) General Remarks

It now seems clear that relativistic bulk motion is a common feature in nuclear components of powerful objects. This must therefore affect the appearance of these objects at some level. Nevertheless, as we have seen, most of the objects in our sample and nearly all the objects that we have mapped have compact, presumably flat-spectrum, cores. In the context of the beaming theories, this suggests either that the cores have broad emission cones or that we have selected objects in which the axis of a narrow emission cone is close to the line of sight. The role of relativistic beaming in these objects is thus far from clear, but this knowledge is essential to understanding the basic physics and statistics of these objects. The determination of the distribution of apparent velocities in this sample, and in other samples selected to minimize the possible effects of beaming on the sample constitution, should help to determine the role of beaming, and lead eventually to a thorough understanding of the physics of these remarkable objects.

The rare exceptions to this unifying picture are the compact S double objects which seem to require an altogether different explanation. These are high-luminosity objects with little if any energy in extended radio components. They must therefore be relatively short-lived, or the energies of the synchrotron-emitting electrons must be dissipated by means other than pure synchrotron radiation (e.g., adiabatic expansion).

VIII. CONCLUSIONS

In this paper we have presented VLBI observations of the compact radio structure in a sample of 65 powerful extragalactic radio sources. This is the largest sample for which such a systematic study has yet been undertaken. We have classified the sources as very compact, compact, asymmetric, compact double, irregular flat-spectrum, compact steep-spectrum, and lobe-dominated. One new result is that we have identified two different types of "compact double" source. Other major results include the following:

- 1. One-sided jets are common features in active galactic nuclei. They are found in every class of object except the compact double objects. The jets typically have steep spectra and are optically thin.
- 2. Compact optically thick cores are found in all objects except the compact S doubles and a few steep-spectrum compact objects; i.e., "naked jets" are rare.
- 3. No two-sided jet has yet been found in an active galactic nucleus (although 3C 390.3 may be an exception to this rule).
- 4. The nuclear jets lie on the same side of the core as the large-scale jets, or, in cases where there are large changes in position angle between the small-scale and the large-scale jet, the two jets connect, sometimes after bending through an angle greater than 90°. No counterexample has been found in which a large-scale jet joins the nucleus on the side opposite a nuclear jet.
- 5. The nuclear jets are fairly highly polarized, with polarizations typically in the range 1%-5%. The nuclear cores have low polarization, typically below 0.5%.

134

7. The compact S double sources seem to be a completely different kind of object. The evidence suggests that the radio structures that we see are not parts of cores or jets, and they have low polarization and variability.

8. A wide variety of morphologies is seen among the compact, asymmetric, steep-spectrum compact, and lobedominated objects. It is therefore remarkable that nearly all of these structures can be resolved into the three basic constituents—nuclear core, contiguous nuclear and large-scale jets, and outer lobes. The complexities and contortions that are seen can all be explained in terms of projection effects, relativistic beaming effects, and interactions with the surrounding medium. It seems therefore that these are all examples of the same underlying mechanism in which power is generated and

collimated into two oppositely directed channels on a scale smaller than a parsec and then propagated by means of a remarkably stable and well-defined channel over distances ranging from a few parsecs to megaparsecs.

This work at the Owens Valley Radio Observatory was supported by National Science Foundation grants AST 82-10259 and AST 85-09822. We are grateful to the US VLBI network and the Max-Planck-Institut für Radioastronomie for generous allocations of observing time, and we wish especially to thank the personnel of the observatories and the Caltech VLBI Processor for their careful attention that made the observations successful. We are also grateful to many colleagues (unfortunately too numerous to name) for providing data in advance of publication and for their stimulating comments on the paper.

APPENDIX

NOTES ON INDIVIDUAL SOURCES

Where necessary, we have assumed $H_0 = 100h \, \mathrm{km \, s^{-1} \, Mpc^{-1}}$ and $q_0 = 0.5$ to convert angles to projected distances. 0016 + 731.—VLA observations at 5 GHz (Perley 1982) show no structure on angular scales between 0".2 and 6" at a level of

0.2 mJy; the fractional polarization is 1.5%. VLBI observations at 5 GHz (Eckart et al. 1986, 1987) show that 70% of the flux density originates a component <3 mas in extent. VLBI observations at 22 GHz (Lawrence et al. 1985) yield a mean visibility of 0.5 between OVRO and Effelsberg.

From our observations there is no evidence of extended structure above a level of 0.1 Jy. The correlated amplitudes and closure phases indicate a slightly resolved and asymmetric structure. We obtained a good fit to the observations with a simple two-component model (Table 4), with a core component slightly extended in P.A. 100° and a weak secondary component 1.7 mas from the core in P.A. 156°.

0040 + 517 (3C 20).—3C 20 is a double radio source with no compact core (an upper limit of about 12 mJy can be placed on the 5 GHz flux density of the core: Laing 1981). Not surprisingly, it was not detected in the finding survey, and we have not attempted to map it.

0108+388.—There is no evidence of any large-scale structure in this object from VLA and Westerbork observations at 5 GHz (Perley 1982; Kapahi 1981). Perley's observations place an upper limit of 0.2 mJy in any component within 6" of the core. Low levels of polarization (0.2%) have been detected at both 1.4 and 5 GHz. The object is not strongly variable (Seielstad, Pearson, and Readhead 1983).

From our observations at 5 GHz, there is no evidence for any structure on angular scales greater than 10 mas, and the flux density of any possible larger feature must be less than 0.1 Jy. A two-component model gave a very good fit to the observations (Table 4). The components are separated in P.A. 60° and both are extended along P.A. 65°-85°. Second-epoch observations (Readhead, Pearson, and Unwin 1984) show no evidence for variations in structure.

0133+476.—There is no evidence of any large-scale structure in this object (Kapahi 1981; Perley 1982). Perley's observations place an upper limit of 0.2 mJy on any structure in the range 0".2-6", and they show that the level of polarization is 1.5% at both 1.4 and 5 GHz. Altschuler (1980) observed a significant rotation in the polarization position angle at 8 GHz during a radio outburst. The source is strongly variable on a time scale of months (Andrew et al. 1978; Seielstad, Pearson, and Readhead 1983). VLBI observations at 5 and 15 GHz (Weiler and Johnston 1980) yielded a visibility of 0.7 between Green Bank and Effelsberg, indicating a size of 0.7 mas. There is also some evidence in their observations for an elongation in P.A. 140°. Marscher and Shaffer (1980) made VLBI observations at 1.7 and 10 GHz; at 1.7 GHz, an elliptical Gaussian model with FWHM 5 mas × 2 mas elongated in P.A. 170° fits well and accounts for all of the flux density of the source; at 10 GHz, an elliptical Gaussian with FWHM 0.8 mas × 0.5 mas elongated in P.A. 123° fits well.

In our observations the closure phases indicate that the object is resolved and asymmetric. A two-component model fits the data well, and shows that there is a resolved component northwest of the unresolved core. A slightly better fit is obtained with the three-component model given in Table 4, which indicates larger structure extending about 10 mas to the west.

0153 + 744.—No large-scale structure has been detected in this object. VLA observations indicate no structure above a level of 0.2 mJy between 0.2 and 6, and they show that the polarization level is low (0.2%) at both 1.4 and 5 GHz (Perley 1982). Eckart et al. (1986, 1987) have made VLBI observations at 1.7 and 5 GHz. At both frequencies they find a double source embedded in a halo. The northern component has an inverted spectrum and is therefore identified with the core. The southern component and halo both have steep spectra. Witzel (1987) has placed an upper limit of 0.03 mas yr⁻¹ ($v/c < 1.3h^{-1}$) on proper motion between the two components.

Our map is in reasonable agreement with the 5 GHz map by Eckart et al.; we find two bright components embedded in a halo. However, it is clear that this is a complex object, and we did not obtain a good fit to the data with simple three- and four-component

models. Our best-fitting model (Table 4) does not give a satisfactory fit to the data, but it does reproduce correctly the gross features of the source. About 25% of the flux density originates in a resolved component larger than 5 mas.

0210 + 860 (3C 61.1).—The central component of this Fanaroff-Riley class II source is weaker than ~ 12 mJy (Laing 1981). We have not attempted to observe it.

0212 + 735.—There is no evidence for extended structure in this object: Antonucci et al. (1986), using the VLA at 1.49 GHz with a 1".2 beam, found no extended emission at a dynamic range of 2700:1. Perley (1982) measured a level of polarization of 2.4% at 5 GHz. The associated optical object is a 19 mag quasar with z = 2.367 (Argue and Sullivan 1980; Lawrence et al. 1986), not a BL Lac object as earlier reported (Biermann et al. 1981). Eckart et al. (1986, 1987) have made VLBI observations at 1.7, 5, and 22 GHz, and found a core-jet structure, with the jet extending 12.5 mas away from the core in P.A. 91° on the 1.7 GHz map. Further VLBI observations (Witzel 1987) have shown that this is a superluminal source.

We obtained a fair fit to our data with a four-component model (Table 4). Our map shows the core-jet structure clearly. Since this object has a number of well-separated bright features, it is an excellent candidate for monitoring superluminal motion.

0220+427 (3C 66B).—3C 66B is a low-luminosity (Fanaroff-Riley class I) radio galaxy. The central core has a flux density of about 0.21 Jy at 5 GHz (Northover 1973); it was not detected in the finding survey, and we did not attempt to map it. (The nearby BL Lac object 3C 66A does contain a milliarcsecond core, but it is too weak for inclusion in the complete sample.)

0314 + 416 (3C 83.1B, NGC 1265).—NGC 1265 is a famous "twin tail" source of Fanaroff-Riley class I. A recent VLA study is that of O'Dea and Owen (1986), which indicates that the nuclear component has a flux density of \sim 25 mJy at 5 GHz. This component has been detected in a VLBI observation at 5 GHz (37 \pm 6 mJy on the Westerbork-Effelsberg baseline: van Breugel et al. 1981), but it is too weak for detection in our finding survey, and it was not included in the mapping observations.

0316+413 (3C 84, NGC 1275).—This complex object has been intensively studied in all accessible spectral bands. A detailed discussion of the compact radio component has been given by Readhead et al. (1983), who showed on the basis of VLBI observations at 22 GHz that it has a core-jet structure extended in the north-south direction, and that the core is situated at the extreme northern end of the jet. At the resolution of the present observations, the structure is dominated by the jet and surrounding halo.

0404 + 768.—This is a steep-spectrum compact radio source, smaller than $\sim 2''$ (Peacock and Wall 1982). We made a short observation in 1980 September, and detected fringes on the most sensitive baseline only. We have not yet attempted to map the source.

0454+844.—There is no evidence for extended structure in this object. Antonucci et al. (1986), using the VLA at 1.49 GHz with a 1.72 beam, found no extended emission at a dynamic range of 1500:1. Perley (1982) found no structure in the range 0.72-6. above 0.3 mJy at 5 GHz, and he found that the object had a polarization level of 3% at both 1.4 and 5 GHz. The object is highly variable on a time scale of months (Seielstad, Pearson, and Readhead 1983). The nearby radio and X-ray source 0450+844 (Biermann et al. 1982) is probably unrelated (Johnston et al. 1984). The associated optical object is a 16.5 mag BL Lac object with unknown redshift (Argue and Sullivan 1980; Biermann et al. 1981). VLBI observations by Eckart et al. (1986, 1987) at 1.7, 5, and 22 GHz show that the object has a double structure with a separation at 5 GHz of 0.52 mas in P.A. 146° (epoch 1979.93).

Our observations are well fitted by a simple double model consisting of a compact component and an extended component (Table 4). Comparing our results with those of Eckart *et al.*, we find that the separation has increased by 0.3 mas in 1.7 yr, implying superluminal motion if the redshift is greater than 1.3.

0538+498 (3C 147).—3C 147 is an archetypal example of a steep-spectrum compact source, and it has been well studied by many workers. In view of this, we did not make 5 GHz observations of this object as part of our survey. Nevertheless, it is part of our complete sample, and we therefore discuss it here for completeness.

The large-scale structure of 3C 147 has been mapped using the VLA at 4.9 and 15.0 GHz by Readhead, Napier, and Bignell (1980), at 15.0 GHz by van Breugel, Miley, and Heckman (1984), and at 5 GHz by Pearson, Perley, and Readhead (1985). There is also a 5 GHz MERLIN map by Wilkinson *et al.* (1984c). In addition there are observations at 81.5 MHz, both by interplanetary scintillations (Readhead and Hewish 1974) and by long-baseline interferometer (Hartas *et al.* 1983). These observations all reveal emission over about 0".5 (2 kpc), with greatest extension in P.A. 20°. There is no evidence of any larger scale structure, so the radio source is presumably much smaller than any host galaxy (in projection, at least). The spectrum has a peak at 120 MHz, and a low-frequency cutoff which is generally attributed to synchrotron self-absorption (Scott and Readhead 1977).

There have been many VLBI observations of 3C 147, including the first hybrid maps to be made by VLBI (Wilkinson et al. 1977). It has been mapped at 327 MHz (Simon et al. 1983), 609 MHz (Wilkinson et al. 1977), 1661 and 1671 MHz (Readhead and Wilkinson 1980; Simon, Readhead, and Wilkinson 1984), and 5 GHz (Preuss et al. 1984). Above 5 GHz it is heavily resolved, and therefore difficult to observe. The VLBI observations at frequencies up to 1671 MHz reveal a one-sided core-jet structure, with the jet extending 0".2 (~1 kpc) to the southwest of the core. At the extreme southwestern end the jet bends through 90° northward over a distance comparable to the width of the jet and then rapidly fades. Such rapid fading in the vicinity of a bend is also seen in 3C 309.1. The width of the jet is ~20 mas (75 pc), and is well resolved. There are a number of distinct regions of higher brightness along the jet. The core is heavily resolved in all directions. It is about 5 mas across and roughly circular. The structure of the core changes at both low frequencies (Simon et al. 1983) and high frequencies (Preuss et al. 1984), but it is complex, and no simple pattern has emerged. The low-frequency variability may be attributable to refractive effects in the interstellar medium (Rickett, Coles, and Bourgois 1984; Blandford and Narayan 1985), or it could represent intrinsic variations enhanced by Dopper boosting (Simon et al. 1983).

The VLA and MERLIN maps show that the "large-scale," 0".5, structure is on the side of the core opposite the jet. There are also faint extensions toward the east. The overall morphology of 3C 147 is mysterious. With its well-collimated jet, diffuse core, and apparent lack of outer lobes, it does not fit into the pattern of either the extended double sources or the compact objects.

0605 + 480 (3C 153).—Any nuclear component in this Fanaroff-Riley class II source is weaker than 5 mJy (Laing 1981). We did not detect it in the finding survey, and have not attempted to map it.

0710+439.—We obtained a relatively poor fit to the data on this source with a simple three-component model (Table 4), but this model does give the flux densities and relative positions of the three major components. Less than 0.1 Jy is unaccounted for in the model; this is consistent with the observations of Kapahi (1981) and Perley (1982), who found less than 0.2 Jy in extended emission on scales 0".2-6".

The map shows that there are three well-separated components, lying very close to a straight line. The component in the middle is extended along the axis; the other components are resolved, but not along any particular line. All three components have similar spectra: there is no obvious flat-spectrum core embedded in any of them (Readhead, Pearson, and Unwin 1984). The source is identified with a faint (20 mag) narrow-emission-line galaxy with redshift z = 0.517 (Lawrence et al. 1986), implying that the maximum size of the source is 25 mas or $100h^{-1}$ pc. The source has a spectrum peaking at about 2 GHz, and has low polarization (0.1% at 5 GHz; Perley 1982) and low variability (Seielstad, Pearson, and Readhead 1983); these properties, along with the similarity of the component spectra, suggest that it should be placed in the class of "compact double steep spectrum" sources, in spite of the fact that it has three components rather than two. The linearity of the source suggests strongly that the components are in some way associated, but it is not obvious that any of them is a "central engine." The point in the source with the flattest spectrum is at the southern end of the central component. It is possible that this point marks the central engine, and that the source is an infant double radio galaxy (Hodges and Mutel 1987), but that is not the only possible interpretation. It is also notable that the southernmost component is rather weak and might have been missed in observations of low dynamic range, in which case we might have been inclined to look for a "central component" midway between the other two. The linear structure makes it plausible to postulate that there is a "jet" in this galaxy, but the three peaks we happen to see may just be accidents—where shock fronts happen to occur, for example. We have studied this source sufficiently well to be able to look for internal motions (Readhead, Pearson, and Unwin 1984). There is no evidence for any changes in component separation in the 2.5 years between our two 5 GHz images. Formally, there is an insignificant subluminal expansion.

0711+356.—VLA observations of this object by Perley (1982) show no evidence for any structure above a level of 0.3 mJy between 0".2 and 6". The radio spectrum has a broad maximum, with a peak at about 2 GHz (Kühr et al. 1981b). It was not significantly variable in the observations of Seielstad, Pearson, and Readhead (1983) on time scales of months to years, but it does vary significantly on a 10 yr timescale. Perley observed a level of polarization of 0.6% at 5 GHz.

We found that a two-component model gives a poor fit to our data, but a fair fit can be obtained with three components, and a good fit with four components (Table 4). There is a strong, very compact component and a one-sided extension to the northwest. Our model fitting shows that the data do require an additional component to the west of northern extension, as seen in the map. We have also made 10 GHz observations of this object (unpublished), which show that the compact southern component has a flat spectrum and should therefore be associated with the core. We have reported second-epoch observations which show that the two major components are not separating, and formally there is an insignificant superluminal contraction (Readhead, Pearson, and Unwin 1984).

0723+679 (3C 179).—3C 179 is a Fanaroff-Riley class II source with a strong central core. An excellent series of VLBI observations revealing superluminal expansion within the core has been conducted by Porcas (1987, and references therein), and we therefore did not include 3C 179 in our observations.

0804+499.—No evidence of extended structure in this object has been found in Westerbork observations (Kapahi 1981) or in VLA observations (Perley 1982), which place an upper limit of 0.2 mJy on structure in the range 0"2-6". The radio source is highly variable on a time scale of a few months (Seielstad, Pearson, and Readhead 1983), and it has a polarization level of 1%-2% at 5 GHz (Perley 1982; Rudnick and Jones 1983).

VLBI observations at 22 GHz (Lawrence et al. 1985) give a visibility of 0.82 on the OVRO-Effelsberg baseline, indicating very compact structure at this frequency. The structure is likewise very compact in our observations, which show a very compact unresolved component with a weak extension to the southeast. The closure phases indicate clearly that the object is extended and asymmetric. A two-component model did not give a good fit, but the three-component model listed in Table 4 gave an excellent fit to both the closure phases and amplitudes.

0809 + 483 (3C 196).—This is a double radio source with an unusual contorted structure which may be due to interaction of a precessing jet with the circumgalactic medium (Lonsdale and Morison 1980, 1983). The flux density of the nuclear component is only ~ 6 mJy (Cawthorne *et al.* 1986, quoting a private communication from R. Laing), so it is not surprising that we did not detect it in our pilot observations. Brown, Broderick, and Mitchell (1986) have made VLBI observations of the compact hot spot in the northern lobe.

0814 + 425.—VLA observations by Perley (1982) reveal a secondary component, of 1.2 mJy, 7".8 from the core in P.A. -40° . This component is double with a separation of 2".8 in P.A. 45° . Perley also measured the level of polarization at 5 GHz to be 0.5%. The total flux density varies by about 50% on a time scale of a few months (Seielstad, Pearson, and Readhead 1983).

We have only a small amount of closure phase data, but they indicate that the object is slightly extended and asymmetric. We obtained a good fit to the data with a two-component model extended in P.A. -31° (Table 4), i.e., toward the secondary component. Observations with higher dynamic range and higher resolution thus may reveal this to be a core-jet source.

0831+557.—The arcsecond-scale emission of this object has been studied with MERLIN (Whyborn et al. 1985). It has a linear triple structure dominated by a core with a steep high-frequency spectrum. The core is straddled by components 5" to the north and 6" to the south. The overal size is 11", corresponding to a projected size of 27 kpc at a redshift of 0.242. Thus the projected distances of the outer components from the core are about 13 kpc, within the host galaxy, but modest deprojection would place them outside the galaxy. The object has also been studied with low-resolution VLBI (Whyborn et al. 1985). In these observations the central component is resolved into two subcomponents separated by 0".16 and aligned with the large-scale structure, and there is evidence of a bridge or jet between the two subcomponents. Our high-resolution VLBI observations resolve the southern subcomponent, revealing it to be amorphous with a roughly circular outline. This is one of the more curious morphologies found in the survey.

We obtained a reasonable fit to our data with the four-component model given in Table 4. This model and the map show a core-jet structure, with the core at the northeastern end of the jet. The jet is roughly aligned with the secondary component seen in the VI A maps

 $0850 + 58\hat{l}$.—Figure 1 shows the first-epoch map of 0850 + 581. We have already published this map and maps from two further epochs (Barthel *et al.* 1986), presenting evidence that this source is the bright core of an extended triple radio source, and shows superluminal motion with an apparent speed $v/c = (4.5 \pm 1.6)h^{-1}c$ along the axis defined by a kiloparsec-scale jet. We obtained a good fit to the first-epoch data with the model given in Table 4.

0859 + 470.—Perley (1982) has detected a faint secondary component in this object at 5 GHz, 1".5 from the core in P.A. -25° , with a flux density of 5.2 mJy. This component is also seen in MERLIN maps at 408 MHz (D. Shone 1986, private communication) along with a weaker component about 1" from the core in P.A. 155°. The flux density varies by about 50% on a time scale of months (Seielstad, Pearson, and Readhead 1983), and the polarization is 2% at 5 GHz (Perley 1982). VLBI observations at 22 GHz by Lawrence et al. (1985) yielded a mean visibility of 0.46 on the OVRO-Effelsberg baseline. Our observations show that the source is clearly resolved in P.A. 0°, and we obtained an excellent fit to the data with a single elliptical Gaussian component with FWHM ~ 2 mas (Table 4).

0906 + 430 (3C 216).—The large-scale structure of 3C 216 has been mapped at the VLA by Schilizzi, Kapahi, and Neff (1982) and by Pearson, Perley, and Readhead (1985). These maps show a bright core straddled by two weaker, resolved components. The core has a flat spectrum and dominates the emission at high frequencies. IPS observations at 81.5 MHz (Readhead and Hewish 1974) show that 50% of the emission originates in components 0".5 in size, and interferometric observations at 81.5 MHz (Hartas et al. 1983) show that about 30% of the emission comes from a region as large as 1'—a projected size of 236 kpc. If this large-scale emission comes from the outer lobes of a classical triple source viewed end-on, then the deprojected size is enormous and the source has some morphological similarities to the giant radio galaxy 3C 236. No other steep-spectrum compact source has been found to have emission on such a large scale, but few such objects have been studied with sufficient sensitivity to detect very faint extended features. This object clearly warrants very high dynamic range VLA observations.

We have made 5 GHz VLBI observations of 3C 216 at three epochs. The first-epoch map (Fig. 1) shows a compact core with a faint extension to the southeast, in a direction almost perpendicular to the large-scale structure. The later maps show superluminal motion at $2.4h^{-1}c$ along this direction, indicative of bulk relativistic motion in the source (Pearson, Readhead, and Barthel 1987). MERLIN and EVN maps (Porcas 1986 and private communication) suggest that the extension seen in the 5 GHz maps is a jet that connects the central core to the western lobe (not the stronger eastern lobe).

The source 3C 216 has several striking similarities to the steep-spectrum compact source 3C 309.1 (1458+718; see the discussion below). The large-scale morphologies are almost identical (Pearson, Perley, and Readhead 1985), the small-scale structure is misaligned with the large-scale structure and shows a compact core and one-sided jet, and there is likely bulk relativistic motion along the jets of both objects. Since very large scale structure has been seen in 3C 216, it is clearly important to make high dynamic range VLA maps to search for such structure in 3C 309.1.

0917 + 458 (3C 219).—This is a Fanaroff-Riley class II source. The central component has a flux density of 51 mJy at 4.9 GHz (Bridle, Perley, and Henriksen 1986), and it was therefore not detected in our VLBI pilot survey. It has, however, been detected at 10.7 GHz using the more sensitive Mark III VLBI system, and has FWHM ≈ 0.5 mas (D. H. Hough, J. O. Burns, and W. A. Christiansen 1987, private communication).

0923 + 392 (4C 39.25).—MERLIN observations of this object by Browne et al. (1982b) reveal a complex structure extending over 5" in P.A. -115° relative to the core. Perley (1982) identified three components, and measured a polarization level of 1% at 5 GHz. The object is not highly variable, but it does show 25% variability over a 10 yr time scale (Seielstad, Pearson, and Readhead 1983).

We obtained a good fit to the data with the two-component model given in Table 4. This model is consistent with the extensive series of observations by Shaffer and Marscher (1987), who find that these two components are stationary and that, subsequent to our observations, a new component has emerged from the western component and is moving toward the eastern component at a superluminal speed.

0945 + 408.—The large-scale structure of this object has been mapped using the VLA by Perley, Fomalont, and Johnston (1980). It consists of a resolved core embedded in a halo 13" (56 kpc) in extent. The core has been mapped using MERLIN by Foley (1982) and is resolved into a very compact core with a one-sided jet extending over 4" (18 kpc). The compact structure revealed by our VLBI observations shows a strong core and a one-sided resolved feature, which may be part of a jet. This feature is roughly perpendicular to the 4" jet; in this respect the object is similar to 3C 216 and 3C 309.1.

The source has a high degree of polarization (6% at 5 GHz) (Perley 1982), and varies on a time scale of a few months (Seielstad, Pearson, and Readhead 1983).

0951+699 (M82, 3C 231).—This irregular galaxy contains a number of discrete, compact radio sources (Unger et al. 1984). The strongest of these, 41.9+58, has been detected in several VLBI observations (e.g., Wilkinson and de Bruyn 1984). This source has been found to have a shell structure and is probably a supernova remnant rather than an active nucleus (Bartel et al. 1987; Wilkinson and de Bruyn 1987). We therefore do not consider it further here.

0954+556.—Although this source was detected in the finding survey, it has not yet been mapped. We are currently analyzing observations made with the EVN.

0954+658.—Although this source was detected in the finding survey, it has not yet been mapped. We are currently analyzing observations made with the EVN.

1003+351 (3C 236).—3C 236 is a giant Fanaroff-Riley class II source with a strong, steep-spectrum central component. We did not include it in our observations, since it has been studied extensively by other workers (Barthel et al. 1985, and references therein).

1031 + 567.—Although this source was detected in the finding survey, it has not yet been mapped. We are currently analyzing observations made with the EVN.

1157 + 752 (3C 268.1).—This is a Fanaroff-Riley class II source with a weak central component (1.7 mJy at 5 GHz; R. A. Laing 1986, private communication; see also Cawthorne et al. 1986). We have not attempted to observe it.

1254 + 476 (3C 280).—This is a Fanaroff-Riley class II source with a weak central component (<10 mJy; Laing 1981). It was not detected in the finding survey.

1358+624.—Although this source was detected in the finding survey, it has not yet been mapped. We are currently analyzing observations made with the EVN.

1409 + 524 (3C 295).—This is a Fanaroff-Riley class II source with a weak central component (<60 mJy; Laing 1981). It was not detected in the finding survey.

1458 + 718 (3C 309.1).—The large-scale structure of 3C 309.1 has been mapped with the VLA (van Breugel, Miley, and Heckman 1984; Pearson, Perley, and Readhead 1985) and with MERLIN (Kus, Wilkinson, and Booth 1981; Wilkinson et al. 1984b). It consists of a very bright core straddled by two weaker components. The separation between the outer components is 2" (8.7 kpc). Thus even the deprojected size is presumably much smaller than that of the parent galaxy.

VLBI observations (Wilkinson et al. 1984b, 1986) reveal a compact core with a fairly flat spectrum, and a jet which extends southward from the core for a distance of 60 mas (260 pc) and then bends eastward through 90° in a distance comparable to the width of the jet, which is about 7 mas (30 pc). The jet fades rapidly at the bend, and, as in the case of 3C 147, there is a bright component at the position where the jet begins to bend. No evidence of a jet is seen on the other side of the core. Wilkinson et al. (1986) show that the low X-ray flux of 3C 309.1 provides evidence for bulk relativistic motion of the radiating material in the brightest knot along the jet; the proper motion of this knot has not yet been measured.

1609 + 660 (3C 330).—This is a Fanaroff-Riley class II source with a weak central component (<75 mJy; Laing 1981). It was not detected in the finding survey.

1624+416.—Kapahi (1981) found no evidence for extended structure in this object on scales larger than 2". Perley (1982) has detected a weak (7 mJy) component 0".7 from the core in P.A. 352°. The object varies on a time scale of months (Seielstad, Pearson, and Readhead 1983) and has a polarization level of 0.2% at 5 GHz (Perley 1982).

We obtained a fair fit to our VLBI data with the two-component model given in Table 4. This model and the map show a structure extending from the core and curving away from the direction defined by the 0.77 secondary component. Owing to instrumental failures (which are not infrequent in VLBI), our data were much more sparse than for most of the objects which we mapped. Nevertheless, the curving core-jet structure is quite clear.

1633+382.—Kapahi (1981) observed this object on the Westerbork synthesis radio telescope (WSRT) and found it to be unresolved. Perley's VLA observations (1982) show it to be essentially unresolved, with a possible short extension 0".2 to the southeast. It is highly variable on time scales of a few months (Seielstad, Pearson, and Readhead 1983) and has a polarization level of about 1.5% at 5 GHz (1982).

There have been a number of VLBI observations of this object. Kellermann *et al.* (1977) fitted their observations with an elliptical Gaussian model with FWHM 0.5 mas \times 0.3 mas extended in P.A. 160°. Marscher and Shaffer (1980) fitted their 1.6 GHz observations with a circular Gaussian with FWHM 1.2 mas.

We obtained an excellent fit to our data with the three-component model given in Table 4. This shows a dominant unresolved core with an extension in P.A. -65° .

1634 + 628 (3C 343).—This compact steep-spectrum object has been mapped with VLBI at 1.66 GHz by Fanti et al. (1985). It has no extended structure and consists of a single complex component 200 mas in diameter. It was not detected in our finding survey, suggesting that any compact feature at 5 GHz is weaker than ~ 300 mJy, and too weak to map with Mark II VLBI on the US network.

1637 + 574.—No high-quality map of the large-scale structure of this object has been published. In observations at 2.7 GHz on the Green Bank interferometer Owen, Porcas, and Neff (1978) detected a secondary component 8" from the core, and Kapahi (1981) observed it at 5 GHz using the WSRT and found it to be elongated by 2" in P.A. 144°. Perley (1982) detected diffuse structures extending approximately 6" northwest and west at 5 GHz. The flux density is highly variable on a time scale of months (Seielstad, Pearson, and Readhead 1983), and the fractional polarization is about 2% at 5 GHz (Perley 1982).

Observations at 22 GHz by Lawrence et al. (1985) yielded a mean visibility of 0.59 on the OVRO-Effelsberg baseline. Our observations were made with stations in the US only and show no strong evidence of extended structure; the closure phases do not depart significantly from zero. The data are reasonably well fitted by a circular Gaussian brightness distribution. We obtained a slightly but not significantly better fit with an elliptical Gaussian (Table 4).

1641 + 399 (3C 345).—This archetypal superluminal source has been the subject of an extensive VLBI study by M. H. Cohen and his collaborators (Biretta, Moore, and Cohen 1986 and references therein). For this reason we did not observe it as part of the survey, although we do include it in the classification and analysis. The large-scale structure consists of a faint halo (Schilizzi and de Bruyn 1983) and a 3" jet (Browne et al. 1982a).

1642+690.—The first-epoch map presented here and our second-epoch map are discussed in detail by Pearson et al. (1986). It is an asymmetric core-jet source showing superluminal expansion. A fair fit which reproduced all the major features in the data was obtained with the three-component model given in Table 4.

1652+398 (Markarian 501).—We obtained a good fit to our data with the three-component core-jet model given in Table 4. Van Breugel and Schilizzi (1986) observed this galaxy on the European VLBI network. Their map, which has lower resolution but greater sensitivity than ours, shows that the jet extends at least 55 mas from the core. In our data, there are variations in the

1739 + 522.—In 1.7 GHz observations on the VLA Perley (1982) and Shone (1986) found that this core-dominated object has a weak secondary component situated 3".5 from the core in P.A. 260°. There is no other evidence for extended structure above a level of 0.3 mJy within 6" of the core. The fractional polarization at 5 GHz is 1% (Perley 1982), and the source is strongly variable (Seielstad, Pearson, and Readhead 1983).

We found that a single component gave a fair fit to our data, but there were systematic deviations in the closure phases of up to 10°, indicating that a more complex, asymmetric model was required. We obtained an excellent fit with the two-component model given in Table 4, which shows that the object is extended in the north-south direction, i.e., roughly orthogonal to the large-scale structure. Observations at 22 GHz by Lawrence et al. (1985) give a mean visibility on the OVRO-Effelsberg baseline of 0.65.

1749 + 701.—VLA observations at 14.9 GHz by O'Dea (1986, private communication) reveal a 5 mJy component 0".4 from the core in P.A. 209°. Perley (1982) found evidence for a 0".4 halo in his 5 GHz observations, and he measured a polarization level of 0.4%. The object is highly variable on a time scale of a few months (Seielstad, Pearson, and Readhead 1983).

Bååth (1984) has made VLBI observations at three epochs, and finds a variable core-jet structure extending in P.A. $\sim 300^{\circ}$. Observations by Eckart *et al.* (1986, 1987) at 1.7 GHz reveal that the object is just resolved at their resolution of 3.4 mas, in P.A. 296°. There is some evidence that the object may be superluminal (Witzel 1987).

Our observations reveal a clear core-jet structure extended in P.A. 296°. The data are fitted well by the two-component model given in Table 4.

1803 + 784.—Antonucci et al. (1986) have made high dynamic range observations of this core-dominated source using the VLA at 1.49 GHz. Their map shows emission extending $\sim 2''$ west and south of the core, and a secondary component of 8.6 mJy $\sim 45''$ south of the core in P.A. 194°. Perley (1982) has measured 5% polarization at 5 GHz. The associated optical object is a 16.4 mag BL Lac object with a redshift of 0.68 (C. R. Lawrence 1987, private communication). A number of other nearby radio and X-ray sources (Biermann et al. 1982) are probably unrelated (Johnston et al. 1984).

VLBI observations by Eckart et al. (1986, 1987) show a core-jet structure at 1.66 GHz extending 30 mas in P.A. 260°. Our map has higher dynamic range than the 5 GHz maps of Eckart et al., and also shows a clear core-jet structure. We obtained a fair fit to the data with the two-component model given in Table 4. Witzel (1987) has placed a subluminal upper limit on any internal proper motion in this source between 1979.9 and 1985.8.

1807+698 (3C 371).—This nearby N galaxy or BL Lac object has been intensively studied in the radio, optical and X-ray bands. A high dynamic range VLA map at 1.7 GHz by Ulvestad and Johnston (1984) reveals that the compact radio source is embedded in an elliptical halo 2' × 1'.5 in extent with the major axis in the east-west direction. Higher resolution VLA observations by Perley, Fomalont, and Johnston (1980) and MERLIN observations by Browne et al. (1982b) reveal a one-sided jet structure, similar to that seen in 3C 120, extending at least 3" in P.A. 240°. The object is highly variable on time scales of a few months (Seielstad, Pearson, and Readhead 1983), and Perley's observations (1982) reveal that it is polarized at the level of 2.7% at 5 GHz.

Numerous VLBI observations have been made of the nucleus of 3C 371. Our first-epoch map, shown here in Figure 1, has already been published (Pearson and Readhead 1981). The map reveals an asymmetric core-jet structure extending 14 mas in P.A. -97° . We obtained a good fit to the data with the four-component model given in Table 4. Our second-epoch map (Readhead, Pearson, and Unwin 1984) has been reanalyzed, together with third-epoch data, by Lind (1987). The source has a complex, variable, core-jet structure, but no clear evidence has been found for superluminal motion. There is, however, evidence for bulk relativistic motion from X-ray and radio variability arguments (Worrall et al. 1984).

1823+568.—MERLIN observations at 408 MHz of this object by Foley (1982) reveal a triple structure extended in P.A. 95°, consisting of a bright core straddled by two components 1".1 and 1".4 away, and connected to the core by bridges of emission. MERLIN 1666 MHz observations (Foley 1982) show a curved jet extending southward from the core and turning to the east 1" south of the core. VLA observations at 5 GHz by O'Dea, Barvainis, and Challis (1986) show the core and the eastern components, but not the western component, indicating that the latter has a steeper spectrum. The object is highly variable on a time scale of a few months and has a polarization level of 5% at 5 GHz (Perley 1982).

Our map shows a one-sided core-jet structure with the jet extending to the south, i.e., in the direction of the large-scale jet. The two-component model given in Table 4 provides a good fit to the data.

1828 + 487 (3C 380).—The large-scale structure of 3C 380 has been mapped a number of times. VLA observations at 5 GHz by Pearson, Perley, and Readhead (1985) show a complex structure extending over 9". This structure is similar to that mapped at 1.7 GHz using MERLIN (Wilkinson et al. 1984a, b; Flatters 1987). Four components can be distinguished in these maps: a compact flat-spectrum core, a short "jet" extending to the northwest, a bright ridge of emission 3" east of the core, and a diffuse halo in which these features are embedded.

The compact component has been studied in several VLBI observations (Readhead and Wilkinson 1980; Wilkinson et al. 1984a), and was observed in the course of this survey. These observations show a compact, flat-spectrum core with a steeper elongated component, generally identified as a "jet," extended 15 mas in P.A. -57° , close to the position angle of the VLA and MERLIN maps (-45°) .

The projected radius of the halo is $20h^{-1}$ kpc; thus even modest deprojection by a factor of 2 would probably place these regions outside the parent galaxy. The spectrum of 3C 380 is steep between 20 MHz and 5 GHz, but flattens above 5 GHz owing to the flat-spectrum core component, which dominates the spectrum at frequencies above 10 GHz.

It is possible that 3C 380 may be a classical triple source seen end-on. There are 20 steep-spectrum double or triple sources in our sample, so that the probability of having one of these objects aligned within 5° of the line of sight is about 10%, which is not too

unlikely for consideration. The size and power of the halo are typical of the outer lobes of powerful triple sources, and the dominance of the flat-spectrum core could be due to relativistic boosting of a weak core component. An alternative possibility, advocated by Wilkinson *et al.* (1984a), is that the morphology of 3C 380 is due to interaction with the interstellar medium. Observations of the broad and narrow optical emission lines may help to discriminate between these two possibilities.

1842+455 (3C 388).—This is a Fanaroff-Riley class II source with a core component of ~ 60 mJy at 4.9 GHz (Burns and Christiansen 1980). This component was too weak for detection in our VLBI pilot survey, but it has been detected at 10.7 GHz using the Mark III system, and its angular size is ~ 0.5 mas (D. H. Hough, J. O. Burns, and W. A. Christiansen 1987, private

communication).

1845 + 797 (3C 390.3).—This is one of the few Fanaroff-Riley class II sources in our sample with a central component that is bright enough to map with the Mark II VLBI system. It has been observed previously by Linfield (1981) and by Preuss et al. (1980). Our observations reveal a dominant component which is just resolved and is extended in P.A. -50°, and a resolved component 4.9 mas away in P.A. -38°, extended in P.A. -43°. The small differences in these position angles are probably not significant. Our observations are in agreement with those of Preuss et al. in showing that there is structure in this object on the northwest side of the core, in contrast to the extension of the core to the southeast found in the higher resolution observations by Linfield at 10.7 GHz. This may therefore be a two-sided nuclear jet. Alef et al. (1987) have made several 5 GHz observations, and have suggested that they indicate superluminal motion of the northeastern component. However, the position of the strongest jet component in their best maps (1980.4 and 1985.4) is almost the same as the position of the northeastern component in our map (1982.2). It seems to us that the data are consistent with no net motion of this component. Further observations spaced more closely will help to clarify this.

1928 + 738.—Recent VLA maps of 1928 + 738 made with very high dynamic range (Rusk and Rusk 1986; Johnston et al. 1987) show that this source, previously thought to be unresolved, is actually an extended double-lobed object. The maps show a curved jet to the south, a counterjet to the north, and a large amorphous lobe of diameter 15" situated 25" north of the core. The whole object is embedded in a halo 1'5 in size.

The first-epoch VLBI map of the core presented here and maps from other epochs are discussed in detail by Eckart *et al.* (1985). The VLBI maps reveal an asymmetric core-jet source showing superluminal motion along a knotty milliarcsecond jet aligned with the southern jet seen in the VLA maps. A five-component model was published by Eckart *et al.*; we have refitted the data and obtain a slightly better fit with the model given in Table 4.

1939 + 605 (3C 401).—This Fanaroff-Riley class II source was not detected in our VLBI pilot survey. The flux density of the central component is ~ 20 mJy (Laing 1981).

1954+513.—VLA observations of this object by O'Dea (1986, private communication) show a possible jet extending 10" north (P.A. 350°) and a component 7" south of a bright unresolved core. The flux density varies by about 20% on time scales of a few months (Seielstad, Pearson, and Readhead 1983), and the fractional polarization is about 0.3% at 5 GHz (Perley 1982).

In our VLBI observations of the core, the closure phases show systematic deviations of up to 10° from zero, indicating that it is resolved and asymmetric. This object has a fairly complex structure extending to the north of the core, and we were unable to obtain a good fit to the closure phase data, although the two-component model given in Table 4 fits the amplitudes well. More observations are needed.

2021+614.—VLA observations by Perley (1982) reveal no structure on scales greater than 0".2 above a level of 0.3 mJy. The source varies only by about 20% on a 10 yr time scale (Seielstad, Pearson, and Readhead 1983), and the polarization is very low (0.1% at 5 GHz; Perley 1982).

Our observations show two almost equal components, placing the object in the "compact double flat spectrum" class. The two components are each resolved into two subcomponents at higher resolution (Bartel et al. 1984a). Two of these are optically thin, one has a flat spectrum, and the other appears to be synchrotron self-absorbed in the frequency range 2.3–8.3 GHz. We obtained a fair fit to the data with the three-component model given in Table 4. By comparison with a second-epoch 5 GHz map, we have placed a subluminal limit on the proper motion between the two bright components, $v = (0.2 \pm 0.2)h^{-1}c$ (Readhead, Pearson, and Unwin 1984).

2153 + 377 (3C 438).—This Fanaroff-Riley class II source has a weak central component (~ 10 mJy; Laing 1981), too weak for detection in our finding survey.

2200 + 420 (BL Lac).—As the archetypal BL Lac object, this source has been studied intensively at all accessible wavelengths, and we do not attempt to review all these observations here. The radio structure is very core-dominated, but a high dynamic range VLA map by Ulvestad and Johnston (1984) reveals a very weak amorphous halo 20" in extent. This halo is slightly elongated in the north-south direction and has a flux density of 40 mJy. No other components are seen above a level of 0.3 mJy at 1.7 GHz and 5 GHz (Perley 1982). The radio source is highly variable on time scales of a few days. At 5 GHz the fractional polarization varies between 1% and 2.5% (Perley 1982; Rudnick and Jones 1982).

There have been numerous VLBI observations of BL Lac (e.g., Kellermann et al. 1977; Weiler and Johnston 1980). Our 5 GHz map shows an asymmetric structure extended in P.A. 180°. We obtained a good fit with the three-component model shown in Table 4. Mutel and Phillips (1987, and references therein) have mapped this object at a number of epochs and found a series of components moving superluminally along this north-south direction.

2229 + 391 (3C 449).—This Fanaroff-Riley class I source has a weak central component that was not detected in our finding survey. VLA observations at 5 GHz (Perley, Willis, and Scott 1979) give the core strength as 37 mJy. The core was detected in a VLBI observation by van Breugel et al. (1981), which showed that it is smaller than 40 mas.

2243 + 394 (3C 452).—This Fanaroff-Riley class II source has a weak central component (130 mJy; Riley and Pooley 1975), too weak for detection in our finding survey.

2342+821.—This is a compact steep-spectrum source (Peacock and Wall 1982). We made a pilot observation of this source in 1980 September, but did not detect it, owing to a typographical error in the position given by Peacock and Wall; the correct position is given in Table 1.

2351+456.—WSRT observations of this object by Kapahi (1979) revealed no structure larger than 2". It is variable on a time scale of a few months (Seielstad, Pearson, and Readhead 1983) and Rudnick and Jones (1982) have measured a fractional polarization of 1.6% at 5 GHz.

We obtained a reasonable fit to all but the shortest baselines with the three-component model given in Table 4. There is clearly

some larger scale structure, since 0.3 Jy is unaccounted for in our model.

2352+495.—This object has no detected radio structure on scales larger than 0."2 (Perley 1982). It exhibits weak variability (15%) on time scales of a few months (Seielstad, Pearson, and Readhead 1983) and 0.2%-0.7% polarization at 5 GHz (Perley 1982).

Our observations show that this is a complex source with a significant amount of emission on scales larger than 10 mas. We tried fitting the data with three- and four-component models, and achieved a fairly poor fit to the data with the three-component model given in Table 4. The map shows two distinct components, one of which has a simple structure while the other is complex. We have classified this as a "compact double steep spectrum" source, but further observations are needed to confirm this classification.

REFERENCES

Alef, W., Götz, M. M. A., Preuss, E., and Kellermann, K. I. 1987, Astr. Ap., submitted. Altschuler, D. R. 1980, A.J., 85, 1559. Andrew, B. H., MacLeod, J. M., Harvey, G. A., and Medd, W. J. 1978, A.J., 83,

Antonucci, R. R. J., Hickson, P., Olszewski, E. W., and Miller, J. S. 1986, A.J.,

92, 1.

Argue, A. N., and Sullivan, C. 1980, M.N.R.A.S., 192, 779.

Bååth, L. B. 1984, in IAU Symposium 110, VLBI and Compact Radio Sources, ed. R. Fanti, K. Kellermann, and G. Setti (Dordrecht: Reidel), p. 127.

Bartel, N., et al. 1984a, Ap. J., 279, 116.

Bartel, N., et al. 1987, Ap. J., 323, 505.

Bartel, N., Shapiro, I. I., Huchra, J. P., and Kühr, H. 1984b, Ap. J., 279, 112.

Porthal B. D. Miley, G. K. Schilizzi R. T. and Preuss F. 1984, Apr. 4n, 140.

Barthel, P. D., Miley, G. K., Schilizzi, R. T., and Preuss, E. 1984, Astr. Ap., 140,

Barthel, P. D., Pearson, T. J., Readhead, A. C. S., and Canzian, B. J. 1986, Ap. J. (Letters), 310, L7.

Barthel, P. D., Schilizzi, R. T., Miley, G. K., Jägers, W. J., and Strom, R. G.

1985, Astr. Ap., 148, 243.
Begelman, M. C., Blandford, R. D., and Rees, M. J. 1984, Rev. Mod. Phys., 56, 255.

Biermann, P., et al. 1981, Ap. J. (Letters), 247, L53. Biermann, P., Fricke, K., Johnston, K. J., Kühr, H., Pauliny-Toth, I. I. K., Strittmatter, P. A., Urbanik, M., and Witzel, A. 1982, Ap. J. (Letters), 252,

Biretta, J. A., Moore, R. L., and Cohen, M. H. 1986, Ap. J., 308, 93

Biretta, J. A., Schneider, D. P., and Gunn, J. E. 1985, A.J., 90, 2508. Blandford, R., and Narayan, R. 1985, M.N.R.A.S., 213, 591.

Biandiord, K., and Narayan, K. 1983, M.N.R.A.S., 213, 391.
Bridle, A. H., Perley, R. A., and Henriksen, R. N. 1986, A.J., 92, 534.
Brown, R. L., Broderick, J. J., and Mitchell, K. J. 1986, Ap. J., 306, 107.
Browne, I. W. A., Clark, R. R., Moore, P. K., Muxlow, T. W. B., Wilkinson, P. N., Cohen, M. H., and Porcas, R. W. 1982a, Nature, 299, 788.
Browne, I. W. A., Orr, M. J. L., Davis, R. J., Foley, A., Muxlow, T. W. B., and Thomasson, P. 1982b, M.N.R.A.S., 198, 673.
Purbidge G. and Crowne, A. H. 1979, Ap. I. Suppl. 40, 583.

Thomasson, P. 1982b, M.N.R.A.S., 198, 6/3.
Burbidge, G., and Crowne, A. H. 1979, Ap. J. Suppl., 40, 583.
Burns, J. O., and Christiansen, W. A. 1980, Nature, 287, 208.
Cawthorne, T. V., Scheuer, P. A. G., Morison, I., and Muxlow, T. W. B. 1986, M.N.R.A.S., 219, 883.
Clark, B. G. 1973, Proc. IEEE, 61, 1242.
Cohen, M. H., et al. 1975, Ap. J., 201, 249.
Cornwell, T. J., and Wilkinson, P. N. 1981, M.N.R.A.S., 196, 1067.
Estart A. Lill, B. Leberton, K. I., Pauliny, Toth, I. I. K. Spencer, I. H. and

Eckart, A., Hill, P. Johnston, K. J., Pauliny-Toth, I. I. K., Spencer, J. H., and

Eckart, A., Hill, P. Johnston, K. J., Fauiniy-Toth, I. I. K., Spencer, J. H., and Witzel, A. 1982, Astr. Ap., 108, 157.
Eckart, A., Witzel, A., Biermann, P., Johnston, K. J., Simon, R., Schalinski, C., and Kühr, H. 1986, Astr. Ap., 168, 17.
— . 1987, Astr. Ap. Suppl., 67, 121.
Eckart, A., Witzel, A., Biermann, P., Pearson, T. J., Readhead, A. C. S., and Johnston, K. J. 1985, Ap. J. (Letters), 296, L23.
Fanaroff, B. L., and Riley, J. M. 1974, M.N.R.A.S., 167, 31P.
Fanti C. Fanti, P. Parma, P. Schiligir, R. T. and van Breugel, W. I. M. 1985.

Fanti, C., Fanti, R., Parma, P., Schilizzi, R. T., and van Breugel, W. J. M. 1985,

Astr. Ap., 143, 292.
Flatters, C. 1987, Nature, 326, 683.
Foley, A. R. 1982, Ph.D. thesis, Victoria University of Manchester.
Hartas, J. S., Rees, W. G., Scott, P. F., and Duffett-Smith, P. J. 1983, M.N.R.A.S., 205, 625.

Hewitt, A., and Burbidge, G. 1987, Ap. J. Suppl., 63, 1. Hodges, M. W., and Mutel, R. L. 1987, in Superluminal Radio Sources, ed. J. A.

Zensus and T. J. Pearson (Cambridge: Cambridge University Press), p. 168. Hodges, M. W., Mutel, R. L., and Phillips, R. B. 1984, A.J., 89, 1327. Hough, D. H., and Readhead, A. C. S. 1987, in Superluminal Radio Sources, ed. J. A. Zensus and T. J. Pearson (Cambridge: Cambridge University Press),

Johnston, K. J., Biermann, P., Eckart, A., Kühr, H., Strittmatter, P. A., Strom, R. G., Witzel, A., and Zensus, A. 1984, Ap. J., 280, 542.
Johnston, K. J., Simon, R. S., Eckart, A., Biermann, P., Schalinski, C., Witzel, A., and Strom, R. G. 1987, Ap. J. (Letters), 313, L85.

Kapahi, V. K. 1979, Astr. Ap., 74, L11.

——. 1981, Astr. Ap. Suppl., 43, 381. Kellermann, K. I., and Pauliny-Toth, I. I. K. 1981, Ann. Rev. Astr. Ap., 19, 373.

Kellermann, K. I., et al. 1977, Ap. J., 211, 658. Kühr, H., Pauliny-Toth, I. I. K., Witzel, A., and Schmidt, J. 1981a, A.J., 86, 854

Kühr, H., Witzel, A., Pauliny-Toth, I. I. K., and Nauber, U. 1981b, Astr. Ap.

Suppl., 45, 367.
Kus, A. J., Wilkinson, P. N., and Booth, R. S. 1981, M.N.R.A.S., 194, 527.

Laing, R. A. 1981, M.N.R.A.S., 195, 261

Lawrence, C. R., Pearson, T. J., Readhead, A. C. S., and Unwin, S. C. 1986, A.J., 91, 494.

Lawrence, C. R., et al. 1985, Ap. J., 296, 458. Lawrence, C. R., Readhead, A. C. S., Pearson, T. J., and Unwin, S. C. 1987, in Superluminal Radio Sources, ed. J. A. Zensus and T. J. Pearson (Cambridge: Cambridge University Press), p. 260.

Lind, K. R. 1987, in Superluminal Radio Sources, ed. J. A. Zensus and T. J. Pearson (Cambridge: Cambridge University Press), p. 180. Linfield, R. 1981, Ap. J., 244, 436. Lonsdale, C. J., and Morison, I. 1980, Nature, 288, 66.

1983, M.N.R.A.S., **203**, 833. Marscher, A. P., and Shaffer, D. B. 1980, A.J., **85**, 668.

Moore, P. K., Browne, I. W. A., Daintree, E. J., Noble, R. G., and Walsh, D. 1981, M.N.R.A.S., 197, 325

Mutel, R. L., and Hodges, M. W. 1986, Ap. J., 307, 472.
Mutel, R. L., Hodges, M. W., and Phillips, R. B. 1985, Ap. J., 290, 86.
Mutel, R. L., and Phillips, R. B. 1987, in Superluminal Radio Sources, ed. J. A. Zensus and T. J. Pearson (Cambridge: Cambridge University Press), p. 60.

Mutel, R. L., Phillips, R. B., and Skuppin, R. 1981, A.J., 86, 1600.

Mutel, R. L., Phillips, R. B., and Skuppin, R. 1981, A.J., 80, 1000.

Northover, K. J. E. 1973, M.N.R.A.S., 165, 369.

O'Dea, C. P., Barvainis, R., and Challis, P. 1986, in IAU Symposium 119, Quasars, ed. G. Swarup and V. K. Kapahi (Dordrecht: Reidel), p. 217.

O'Dea, C. P., and Owen, F. N. 1986, Ap. J., 301, 841.

Owen, F. N., Porcas, R. W., and Neff, S. G. 1978, A.J., 83, 1009.

Pauliny-Toth, I. I. K., Witzel, A., Preuss, E., Kühr, H., Kellermann, K. I., Fomalont, E. B., and Davis, M. M. 1978, A.J., 83, 451 (S4).

Peacock, J. A., Perryman, M. A. C., Longair, M. S., Gunn, J. E., and Westphal, J. A. 1981, M.N.R.A.S., 194, 601.

Ap. J. (Letters), 300, L25.
Pearson, T. J., Perley, R. A., and Readhead, A. C. S. 1985, A.J., 90, 738.

R. Fanti, K. Kellermann, and G. Setti (Dordrecht: Reidel), p. 15.

— . 1984b, Ann. Rev. Astr. Ap., 22, 97.

Pearson, T. J., Readhead, A. C. S., and Barthel, P. D. 1987, in Superluminal Radio Sources, ed. J. A. Zensus and T. J. Pearson (Cambridge: Cambridge University Press), p. 94. Perley, R. A. 1982, A.J., 87, 859

Perley, R. A., Bridle, A. H., Willis, A. G., and Fomalont, E. B. 1980, A.J., 85,

Perley, R. A., Fomalont, E. B., and Johnston, K. J. 1980, A.J., 85, 649.

Perley, R. A., Willis, A. G., and Scott, J. S. 1979, *Nature*, **281**, 437. Phillips, R. B., and Mutel, R. L. 1980, *Ap. J.*, **236**, 89.

. 1981, Ap. J., 244, 19

Phinney, E. S. 1985, in Astrophysics of Active Galaxies and Quasi-stellar Objects, ed. J. S. Miller (Mill Valley: University Science Books), p. 453.

Porcas, R. W. 1981, Nature, 294, 47.

1986, in IAU Symposium 119, Quasars, ed. G. Swarup and V. K. Kapahi (Dordrecht: Reidel), p. 131.

1987, in Superluminal Radio Sources, ed. J. A. Zensus and T. J. Pearson (Cambridge: Cambridge University Press), p. 12.

1988ApJ...328..114P

Preuss, E., Alef, W., Whyborn, N., Wilkinson, P. N., and Kellermann, K. I. 1984, in *IAU Symposium 110*, *VLBI and Compact Radio Sources*, ed. R. Fanti, K. Kellermann, and G. Setti (Dordrecht: Reidel), p. 29.

Preuss, E., Kellermann, K. I., Pauliny-Toth, I. I. K., and Shaffer, D. B. 1980,

Ap. J. (Letters), 240, L7.

Readhead, A. C. S., and Hewish, A. 1974, Mem. R.A.S., 78, 1.

Readhead, A. C. S., Hough, D. H., Ewing, M. S., Walker, R. C., and Romney, J. D. 1983, Ap. J., 265, 107.

Readhead, A. C. S., Napier, P. J., and Bignell, R. C. 1980, Ap. J. (Letters), 237,

Readhead, A. C. S., Pearson, T. J., and Barthel, P. D. 1987, in IAU Symposium 129, The Impact of VLBI on Astrophysics and Geophysics, ed. M. J. Reid and J. M. Moran (Dordrecht: Reidel), in press.

Readhead, A. C. S., Pearson, T. J., and Unwin, S. C. 1984, in IAU Symposium 110, VLBI and Compact Radio Sources, ed. R. Fanti, K. Kellermann, and

G. Setti (Dordrecht: Reidel), p. 131.

J. A. Zensus and T. J. Pearson (Cambridge: Cambridge University Press),

Rudnick, L., and Jones, T. W. 1982, Ap. J., 255, 39.

1983, A.J., 88, 518.

Rusk, R. 1987, in IAU Symposium 129, The Impact of VLBI on Astrophysics and Geophysics, ed. M. J. Reid and J. M. Moran (Dordrecht: Reidel), in

Rusk, R., and Rusk, A. C. M. 1986, Canadian J. Phys., 64, 440. Rusk, R., and Seaquist, E. R. 1985, A.J., 90, 30. Schilizzi, R. T., and de Bruyn, A. G. 1983, Nature, 303, 26.

Schilizzi, R. T., Kapahi, V. K., and Neff, S. G. 1982, J. Ap. Astr., 3, 173. Schwab, F. R., and Cotton, W. D. 1983, A.J., 88, 688. Scott, M. A., and Readhead, A. C. S. 1977, M.N.R.A.S., 180, 539.

Seielstad, G. A., Pearson, T. J., and Readhead, A. C. S. 1983, Pub. A.S.P., 95,

Shaffer, D. B., and Marscher, A. P. 1987, in Superluminal Radio Sources, ed. J. A. Zensus and T. J. Pearson (Cambridge: Cambridge University Press),

Shone, D. L. 1986, Ph.D. thesis, Victoria University of Manchester.

Simon, R. S. 1982, Ph.D. thesis, California Institute of Technology.

Simon, R. S., Readhead, A. C. S., Moffet, A. T., Wilkinson, P. N., Allen, B., and Burke, B. F. 1983, Nature, 302, 487.
Simon, R. S., Readhead, A. C. S., and Wilkinson, P. N. 1984, in IAU Symposium 110, VLBI and Compact Radio Sources, ed. R. Fanti, K. Kellermann, and G. Setti (Dodrecht, Bridel). and G. Setti (Dordrecht: Reidel), p. 111. Spinrad, H. 1982, *Pub. A.S.P.*, **94**, 397.

Spinrad, H. 1982, Pub. A.S.P., 94, 397.
Ulvestad, J. S., and Johnston, K. J. 1984, A.J., 89, 189.
Ulvestad, J. S., Johnston, K. J., and Weiler, K. W. 1983, Ap. J., 266, 18.
Unger, S. W., Pedlar, A., Axon, D. J., Wilkinson, P. N., and Appleton, P. N. 1984, M.N.R.A.S., 211, 783.
van Breugel, W., Miley, G., and Heckman, T. 1984, A.J., 89, 5.
van Breugel, W., and Schilizzi, R. 1986, Ap. J., 301, 834.
van Breugel, W. J. M., Schilizzi, R. T., Hummel, E., and Kapahi, V. K. 1981, Actr Ap. 96, 310.

van Breugel, W. J. M., Schillzel, R. I., Flummer, E., and Kapani, V. K. 1901, Astr. Ap., 96, 310.

Weiler, K. W., and Johnston, K. J. 1980, M.N.R.A.S., 190, 269.

Whyborn, N. D., Browne, I. W. A., Wilkinson, P. N., Porcas, R. W., and Spinrad, H. 1985, M.N.R.A.S., 214, 55.

Wilkinson, P. N., Booth, R. S., Cornwell, T. J., and Clark, R. R. 1984a, Nature, 200 210

Wilkinson, P. N., Cornwell, T. J., Kus, A. J., Readhead, A. C. S., and Pearson, T. J. 1984b, in NRAO Workshop No. 9, Physics of Energy Transport in Extragalactic Radio Sources, ed. A. H. Bridle and J. A. Eilek (Green Bank:

T. J. 1986, in IAU Symposium 119, Quasars, ed. G. Swarup and V. K. Kapahi (Dordrecht: Reidel), p. 165.

Wilkinson, P. N., Readhead, A. C. S., Purcell, G. H., and Anderson, B. 1977, *Nature*, 269, 764.

Wilkinson, P. N., Spencer, R. E., Readhead, A. C. S., Pearson, T. J., and Simon, R. S. 1984c, in *IAU Symposium 110*, VLBI and Compact Radio Sources, ed. R. Fanti, K. Kellermann, and G. Setti (Dordrecht: Reidel), p. 25.

Witzel, A. 1987, in Superluminal Radio Sources, ed. J. A. Zensus and T. J.

Pearson (Cambridge: Cambridge University Press), p. 83.
Worrall, D. M., et al. 1984, Ap. J., 278, 521.
Zensus, J. A., and Porcas, R. W. 1986, in IAU Symposium 119, Quasars, ed. G. Swarup and V. K. Kapahi (Dordrecht: Reidel), p. 167.

T. J. Pearson and A. C. S. Readhead: Owens Valley Radio Observatory, 105-24 California Institute of Technology, Pasadena, CA 91125